Real-time Energy Management of PHEVs with Supercapacitor Using Nonlinear Model Predictive Control

by

Mohammad Hassanpour

A thesis
presented to the University of Waterloo
in fulfillment of the
thesis requirement for the degree of
Master of Applied Science
in
Systems Design Engineering

Waterloo, Ontario, Canada, 2018

I hereby declare that I am the sole author of this thesis. This is a true copy of the thesis, including any required final revisions, as accepted by my examiners.

I understand that my thesis may be made electronically available to the public.

Abstract

The earth is facing the global warming phenomenon these days, and one of its main contributors is greenhouse gas emission. As transportation produces an enormous portion of greenhouse gasses and also due to the increasing price of oil, automotive companies are now motivated more than ever to manufacture more hybrid vehicles compared to conventional vehicles.

Although hybrid vehicles decrease the fuel consumption and greenhouse gas emissions, the cost of ownership and short lifespan of batteries have always been a drawback for them. Comparing the merits and demerits of batteries and Supercapacitors (SC) convinced researchers to use a combination of both to utilize vehicles with, as none of them could replace the other completely. An energy management strategy is crucial for maximizing benefits from utilizing vehicles with a hybrid energy storage system.

This study includes modelling an SC module and developing Nonlinear Model Predictive Control (NMPC) strategies for the Toyota Prius Plug-in Hybrid Electric Vehicle (PHEV) with SC. Enhancements in vehicles processing units have absorbed attentions into more complex energy management strategies like MPC.

Model-in-the-Loop (MIL) simulations and Hardware-in-the-Loop (HIL) tests investigate the performance of the proposed strategies. HIL tests results suggest the prediction horizon lengths for that the proposed controllers can be real-time implementable. Moreover, the MIL simulations results investigate the performances of fuel consumption and lifespan of the battery. Repeating the MIL simulations for different scenarios guarantees the performance enhancement regardless of driver's behaviour.

Using Nonlinear Model Predictive Controller (NMPC) as Energy Management Strategy (EMS) in this study shows improvements in fuel consumption and lifespan of the battery

up to **7.4%** and **62%**, respectively. While hybridizing Energy Storage System (ESS) with Supercapacitor (SC) can achieve up to **47%** reduction in the battery load.

Acknowledgements

I would like to thank my supervisor, Prof. Nasser L. Azad, for his insight and guidance. This research was not possible without his support.

I would also like to thank my colleagues and friends in SHEVS Lab, M. Vajedi, S. Tajeddin, P. Golchoubian, S. Ekhtiari, Y. Masoudi, B. Sakhdari, whom I have used their valuable experiences.

I acknowledge the NSERC and Toyota for financially supporting this work.

Dedication

To my brother, Soroosh, who has always been by my side, and to my awesome parents and friends.

Table of Contents

List of Tables x

List of Figures xi

Abbreviations xiii

1 Introduction 1

1.1 Motivation and Challenges 1

1.2 Problem Statement and Proposed Approach 3

1.3 Thesis Organization 5

2 Literature Review and Background 6

2.1 Battery-SC HESS Configuration 6

2.2 Supercapacitor Modelling 8

2.3 Energy Management Controllers 10

2.4 Model Predictive Control 11

2.5 Summary 13

3 Modelling **14**

3.1 High-fidelity Model (Autonomie) 14

3.2 Supercapacitor Model 15

3.3 Control-oriented Model 18

3.4 Summary 30

4 Energy Management Strategy Design **31**

4.1 Rule-based Controllers 32

4.1.1 High-level Controller (Engine-HESS) 32

4.1.2 Low-level Controller (Battery-SC) 34

4.2 Model Predictive Controllers 34

4.2.1 High-level Controller (Engine-HESS) 35

4.2.2 Low-level Controller (Battery-SC) 36

4.3 Summary 39

5 Energy Management Strategy Evaluation **40**

5.1 Hardware-in-the-Loop Testing 41

5.2 Model-in-the-Loop Simulation 44

5.3 Summary 54

6 Conclusion and Future Work **55**

6.1 Contributions 56

6.2 Future Steps 56

References 58

List of Tables

3.1 Specification of Maxwell BCAP0010 SC Cell 17

3.2 Parameters of Complete Model for Maxwell BCAP0010 SC[1] 17

3.3 Parameters of Toyota Prius Battery Pack 20

3.4 Parameters of Fuel Consumption Control-oriented Model in Eq. 3.3 22

5.1 HIL Components Specification 42

5.2 Estimated Turnaround Time Based on Measured Turnaround Time 45

5.3 MIL Simulation Results (Fuel Consumption) 45

5.4 MIL Simulation Results (Battery Load) 46

List of Figures

2.1 Simple Parallel Configuration 7

2.2 Common Battery SC Configuration with One Converter 8

2.3 More Complex Battery SC Configuration with Two Converters 8

2.4 Series SC Model Proposed in [2] 9

2.5 Parallel SC Model Proposed in [3] 10

2.6 Complete SC Model Proposed in [1] 11

2.7 Model Predictive Control Principle 12

2.8 Different Model Predictive Control Types Based on Future Power Prediction[4] 13

3.1 Prius Power-split Configuration 15

3.2 Autonomie High-fidelity Model of Toyota Prius without SC 16

3.3 Autonomie High-fidelity Model of Toyota Prius with SC 18

3.4 Control-oriented Model for Battery (Left) and SC (Right) 19

3.5 Optimal Speed of the Engine for Different Powers 21

3.6 Engine Fuel Consumption for Different Torques and Speeds 22

3.7 Sample Engine Power for Control-oriented Verification 23
3.8 Sample Battery Power for Control-oriented Verification 24
3.9 Sample SC Power for Control-oriented Verification 25
3.10 Fuel Consumption from High-fidelity and Control-oriented Model Comparison 26
3.11 Battery High-fidelity and Control-oriented Model Comparison 27
3.12 Battery High-fidelity and Control-oriented Model Error over Time 28
3.13 SC High-fidelity and Control-oriented Model Comparison 29

4.1 Schematic of the High-level and Low-level Controllers Relation 32
4.2 Autonomie High-level RBC Algorithm 33
4.3 Low-level RBC Algorithm [5] 35

5.1 Schematic of HIL Setup 41
5.2 Turnaround Times in One HIL Test 43
5.3 Turnaround Time for Different Prediction Horizon Lengths 44
5.4 Fuel Consumption Comparison for 2xWLTP Drive Cycle 48
5.5 Fuel Consumption Comparison for 3xHWFET Drive Cycle 49
5.6 Fuel Consumption Comparison for 3xUDDS Drive Cycle 50
5.7 Battery Load Comparison for 2xWLTP Drive Cycle 51
5.8 Battery Load Comparison for 3xHWFET Drive Cycle 52
5.9 Battery Load Comparison for 3xUUDS Drive Cycle 53

Abbreviations

CAN Controller Area Network 37

ECU Electronic Control unit 37

ESS Enrgy Storage System 5

HESS Hybrid Energy Storage System 3

HIL Hardware-in-the-Loop 4

LMPC Linear Model Predictive Controller 3

MIL Model-in-the-Loop 4

MPC Model Predictive Control 2

NMPC Nonlinear Model Predictive Controller 3

PC Personal Computer 37

PHEV Plug-in Hybrid Electric Vehicle 2

RBC Rule-based Controller 3

RMS Root Mean Square 35

SC Supercapacitor 2

SOC State of the Charge 17

Chapter 1

Introduction

Transportation is one of the most significant contributors to the greenhouse gas emission in the world[6, 7]. Researchers suggest the greenhouse gas emissions will rise 80% between 2007 and 2030[8]. Therefore, hybridizing vehicles to reduce fossil fuel consumption has absorbed more attention in the automotive industry than ever[9, 10, 11]. However, there are many challenges that the automotive companies are facing in their paths toward substituting the conventional cars with hybrid cars.

1.1 Motivation and Challenges

Aside from all the benefits of hybrid vehicles[12], issues like the short life of batteries and increased vehicle price are the drawbacks that researchers all around the world are committed to solving.

The fluctuations in batteries output current and high power demands from batteries usually make the battery inefficient and reduce the lifespan of the battery. Therefore, many

studies have been conducted to replace the batteries with Supercapacitor (SC). SCs have thousand times longer lifespans compared to batteries[13]. The low internal resistance of the SCs will reduce the energy loss and will increase the efficiency. Also, SCs have higher power density due to the lower internal resistance. The high power density of the SC Allows the controller of the vehicle to be able to perform more efficiently. However, SCs have a thousand times lower energy density which means that to for the same amount of electric energy stored SCs weigh much more[14]. Consequently, researchers proposed many hybrid configurations of battery and SCs to utilize merits of each.

The researchers' logic behind using the battery and SC instead of having two batteries is that a second battery increases the financial cost of the vehicle ownership compared to adding SC to the system. Also, batteries cannot provide the same amount of power as SCs instantaneously. Li-ion batteries are usually used in the automotive industry as they outperform all other types of batteries and since the comparisons are between SC and Li-ion batteries.

Researchers proposed different energy management strategies for Plug-in Hybrid Electric Vehicle (PHEV) with SCs in the literature[14, ?]. However, there is still vast potential for improving the performance of the PHEVs with SCs.

Model Predictive Control (MPC) is an optimal control strategy, used as energy management strategy in vehicles, where the decision is made based on the consequences of the decision over a receding prediction horizon. Many studies in automotive applications [15, 16] have shown the potentials in this strategy. MPC can exploit the knowledge of future information about traffic, pedestrian presence, and preceding vehicles velocity to provide a more optimal input for the system.

Although the more efficient performance of MPC is a known fact, the computational

cost of this method has always been a drawback for it. Moreover, the challenge gets more intense with increasing the prediction horizon length, increasing the non-linearity of the system, and increasing the number states, inputs, and constraints of the problem. With improvements in the processing units in vehicles, the MPC has absorbed more attention from researchers than ever since the real-time implementation of MPC strategies has now become feasible.

This study develops real-time Linear Model Predictive Controller (LMPC) and Nonlinear Model Predictive Controller (NMPC) for Toyota Prius PHEV with SC. Also, compares the performance of the proposed strategies to benchmark rule-based strategies presented in the literature.

1.2 Problem Statement and Proposed Approach

The objective of this study is to design real-time model predictive energy management controllers for PHEVs with SC to reduce the fuel consumption and improve the lifespan of the battery. The performance of the proposed controller should have improved compared to benchmark Rule-based Controller (RBC) for Toyota Prius vehicle with Hybrid Energy Storage System (HESS). The steps taken for achieving this objective are as follows:

- **Supercapacitor Modelling:** An SC model needs to be modelled and the configuration of the HESS should be decided. The SC model should be adequately accurate and fast for simulations. The parameters of the SC model should be identified for a specific SC cell. Also, The high-fidelity model of the Toyota Prius should be integrated with the SC model.

- **Control-oriented Modelling:** For designing real-time MPCs, a fast, simple, yet accurate enough model is needed. This model should be able to capture the dynamics of the high-fidelity model. The validity of this control-oriented model should be verified upon the high-fidelity model.

- **Energy Management Strategy Design:** Firstly, benchmark RBCs should be designed for investigation of the impact of adding an SC model. Also, these RBCs will be used as benchmarks for MPCs to outperform. MPCs are developed, trained, and robust calibrated to improve fuel consumption and lifespan of the battery.

- **Energy Management Strategy Evaluation:** Lastly, Hardware-in-the-Loop (HIL) tests and Model-in-the-Loop (MIL) simulations are implemented. The length of the prediction horizon for the controller will be distinguished using the HIL test results and the criteria of real-time performance for vehicle control. Also, by tuning the weights of the MPCs, a set of weights will be found with which the MPCs can outperform the benchmark RBCs. The simulations will be repeated for different driving cycles to make sure that the improvements are not dependant on the driving scenario.

1.3 Thesis Organization

This thesis consists of 6 chapters. Chapter 2 reviews the literature for some concepts used in this thesis and also presents a summary of similar works that have been done before. Chapter 3 talks about the high-fidelity and control-oriented model which has been used throughout the thesis for designing controllers, simulations, and evaluations. This chapter also validates the control-oriented model with the high-fidelity model. Chapter 4 covers the energy management systems for the vehicle including RBCs which have been used as benchmarks and MPC controllers. Chapter 5 presents the evaluations from the MIL simulations and HIL experiments and the performance improvements due to substituting RBCs with MPCs. In the end, Chapter 6 wraps the thesis with future steps and a discussion.

Chapter 2

Literature Review and Background

This chapter presents some descriptions of some critical concepts which the author has used in this thesis. It also provides a review of different proposed energy management controllers in the literature. Various ways of modelling an SC is discussed, and benefits of the chosen architecture for hybridizing battery model with SC model are also described.

This chapter is organized as follows: Section 2.1 describes different configurations for hybridizing Enrgy Storage System (ESS) of vehicles. Section 2.2 introduces different proposed models for modelling a SC. Section 2.3 discusses energy management controllers for HESS. Section 2.4 covers the concept of MPC, and some challenges and improvements are discussed. In the end, a summary of the chapter is provided in section 2.5.

2.1 Battery-SC HESS Configuration

There is a trade-off between the complexity, cost, and the degrees of freedom in implemented control strategies in different configurations of HESSs. A review on different con-

figurations can be found in the literature [17].

The simplest and most cost-efficient configuration is the one where battery and SC models are parallel without any converter in between. Although, this approach does not add a degree of freedom to the system and SC works as a low-pass filter [18]. Fig. 2.1 schematically shows this configuration.

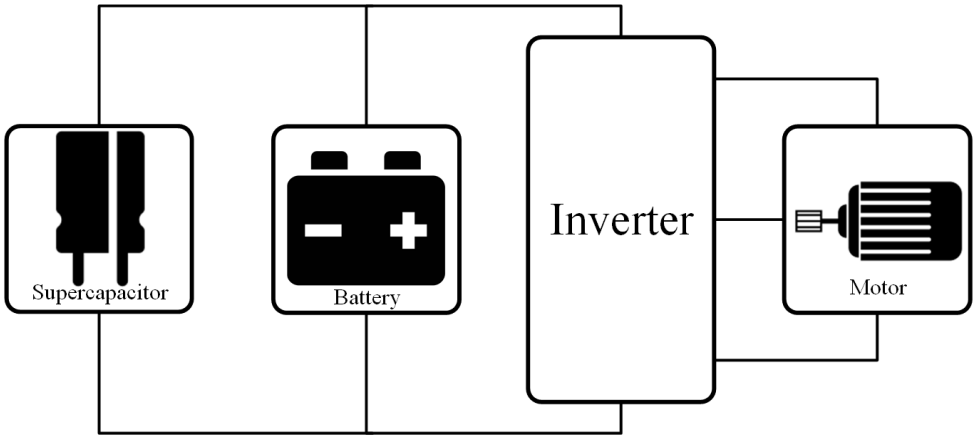

Figure 2.1: Simple Parallel Configuration

Adding a bidirectional DC/DC converter in the previous configuration, as Fig. 2.2 suggests, makes the configuration to have an extra degree of freedom and also does not add too much to the complexity and the cost of the configuration. Reasons mentioned above make this configuration the most common one in the literature [19, 17].

If the application of hybridizing ESSs needs, adding another bidirectional DC/DC converter makes voltages of both SC and battery independent from the DC bus. It also should be mentioned that adding another DC/DC converter increases the cost of the configuration. This configuration is shown in Fig. 2.3. More complex configurations with additional converters are also introduced in the literature[20, 21]. These configurations are more complex and financially more inefficient but more accurate.

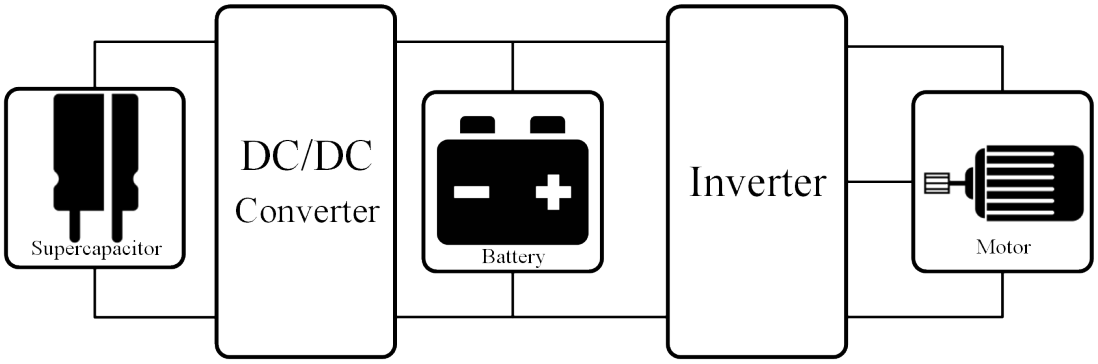

Figure 2.2: Common Battery SC Configuration with One Converter

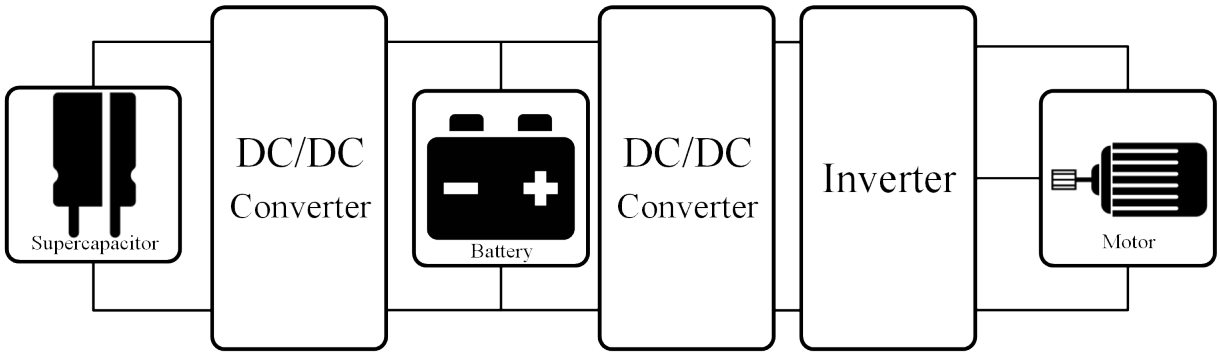

Figure 2.3: More Complex Battery SC Configuration with Two Converters

2.2 Supercapacitor Modelling

SC which is also called "double layer capacitor" [22], will behave differently in charging and discharging situations [23]. Numerous ways are introduced in the literature for SC modelling [3, 2, 1].

The series model consists of one branch with an infinite number of elements. This model can accurately represent the behaviour of the SC for low frequencies. The schematic of this model is shown in Fig. 2.4. The parameters of this model are identified through frequency analysis of the cell. These measurements need special instrumentation, a spectroscope.

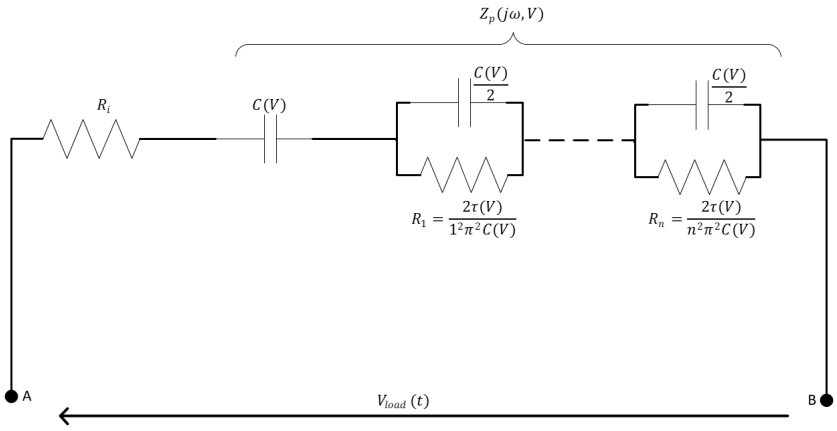

Figure 2.4: Series SC Model Proposed in [2]

The parallel model, which is schematically shown in Fig. 2.5, has three parallel branches. This model can successfully represent the redistribution phenomenon, nonlinear dynamics of the SC, and leakage. This model's accuracy is acceptable for high frequencies. Parameters of this model can be identified for a specific cell through a constant current charge/discharge test and the manufacturer data sheet.

The complete model introduced in [1] is a combination of series and parallel models. The complete model can represent all the phenomena that parallel model can represent, and the parameters of this model also can be identified through a constant charge test and manufacturer data sheet. Also, the complete model successfully can represent the dynamics of the SC in both high and low frequencies. Fig. 2.6 shows the schematic of the complete model.

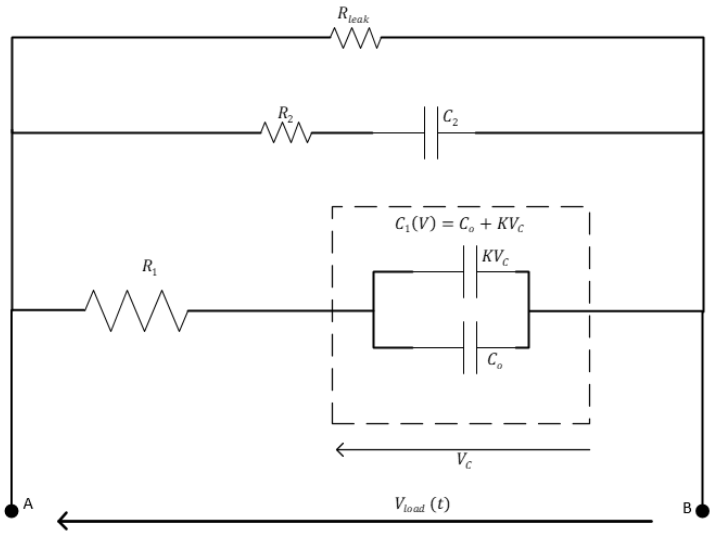

Figure 2.5: Parallel SC Model Proposed in [3]

2.3 Energy Management Controllers

The two major of energy management strategies in the literature are rule-based methods and optimization-based approaches [24, 25, 26, 27]. In rule-based approaches, a set of rules or predefined sets of action for specific situations situations are used and the implementation of those rules are simple. Therefore, the controller's output is just related to the current situation and it usually does not yield the optimal output from the system. Unlike RBCs, optimization-based controllers can use future information of the trip to come up with better solutions. These methods are also called route-based in the literature [28].

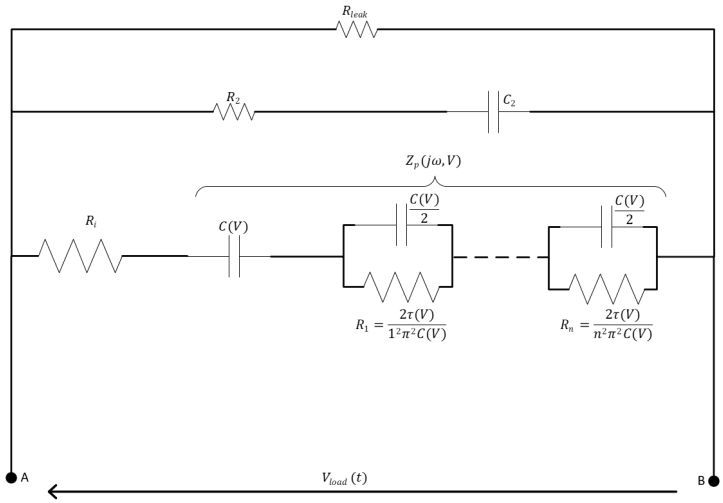

Figure 2.6: Complete SC Model Proposed in [1]

2.4 Model Predictive Control

MPC which is also called receding horizon control [29] is a optimization-based control strategy which also can handle constraints acting on states or inputs. Fig. 2.7 visualizes the principle of the MPC strategy. MPC strategies for the hybrid vehicles with SC usually try to minimize the load on the battery and increase the lifespan.

MPC can be divided into different types based on the prediction over the prediction horizon. Fig. 2.8 introduces five of different MPC categories. In prescient MPC, it is assumes that the full knowledge of future is available [30, 31]. Although prescient MPC yields the best result, it is not always possible to make this assumption. Frozen-time MPC assumes that the varying parameter of the systems stays constant over the prediction horizon[32, 30]. Exponential-varying MPC assumes that the varying parameter decays exponentially over the prediction horizon [33, 34]. Stochastic MPC is utilized with some probability functions that can provide the future information with a probability related

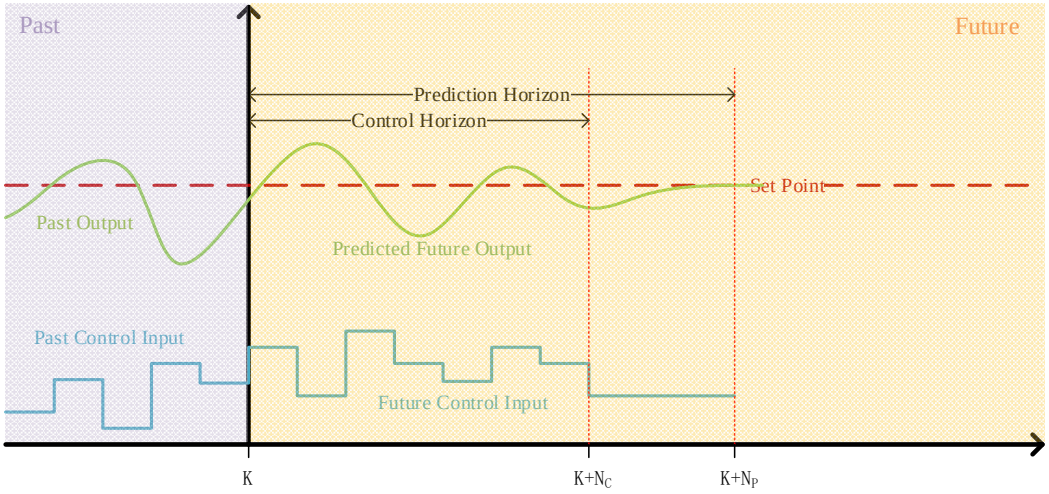

Figure 2.7: Model Predictive Control Principle

to each scenario [35, 36, 37, 38]. Artificial intelligent MPC is equipped with different artificial intelligent tools that provide the future information for MPC over the prediction horizon[35, 39, 40, 41].

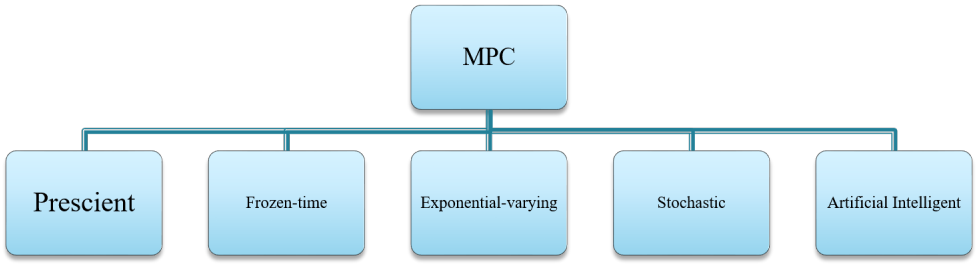

Figure 2.8: Different Model Predictive Control Types Based on Future Power Prediction[4]

2.5 Summary

Some main concepts and similar works were discussed in this chapter, so we have a better insight into the potentials of this problem. First, the complexity, cost, and the degrees of freedom of the different possible configurations of integrating battery and SC are discussed. Also, the proposed models for SC in the literature are introduced. Then, the energy management controllers which has been used for different purposes are presented. Finally, different MPC methods are listed to give a better vision about the potential benefits that exploiting the MPC method as an energy management controller might yield.

Chapter 3

Modelling

In this chapter, the model which was used to design and implement different control strategies is presented. The model consists of a high-fidelity model of the Toyota Prius and the SC model. The SC model was integrated with the high-fidelity model of the vehicle to investigate the potentials in hybridizing ESS of the vehicle.

This chapter is organized as follows: Section 3.1 explains the Autonomie high-fidelity model and the subsystems in it. Section 3.2 talks about the SC model and the HESS configuration. In section 3.3, The control-oriented model for the purpose of designing controllers is presented. In the end, a summary of the model which will be used for all of the simulations and experiments throughout this thesis is in section 3.4.

3.1 High-fidelity Model (Autonomie)

Toyota Prius is a PHEV. This vehicle uses a special power-split configuration. The power-split system, as shown in Fig. 3.1, connects motor, generator, and engine with planetary

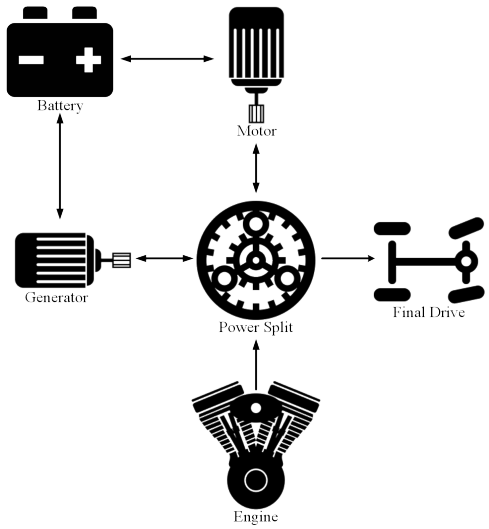

Figure 3.1: Prius Power-split Configuration

gears. Systems mentioned above enable the engine to always operate in the optimum points among the set of points that can produce the same amount of power.

Argonne National Lab developed the high-fidelity model of the Toyota Prius vehicle is in Autonomie software. This model has been validated by numerous simulations in [42].

This high-fidelity model consists of four main subsystems: Driver, Environment, Energy Management Controller, and Powertrain. The powertrain includes models of battery, motor, generator, engine, and chassis. Fig. 3.2 schematically shows the high-fidelity model block diagram and the data flow in this model.

3.2 Supercapacitor Model

The configuration chosen for this study among those which has been introduced in the literature is the parallel configuration with one DC/DC converter as shown in Fig. 2.2.

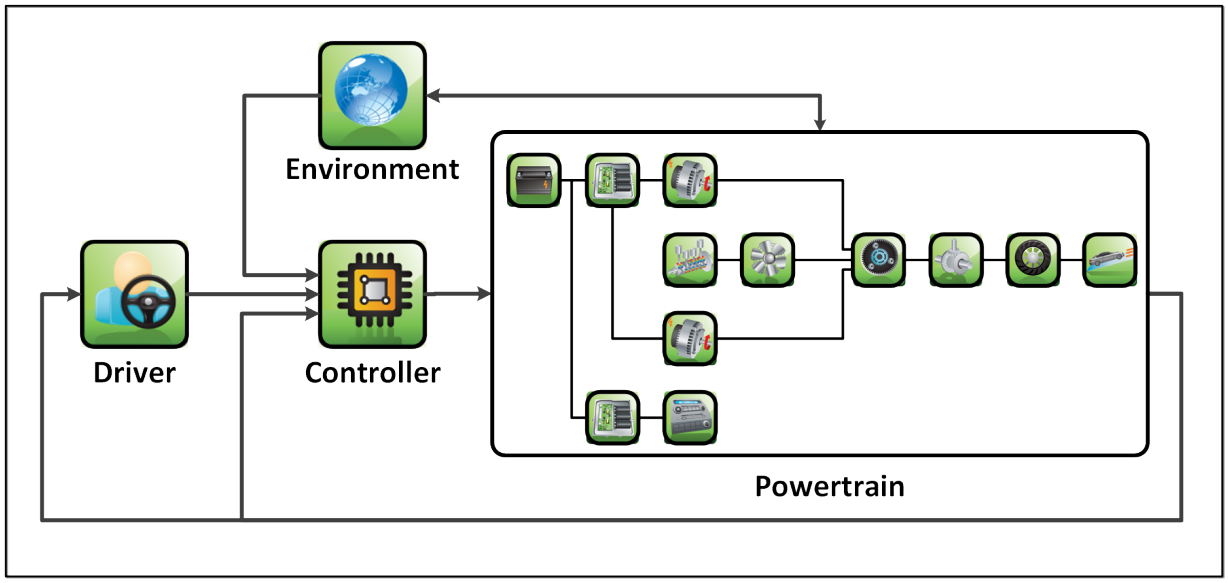

Figure 3.2: Autonomie High-fidelity Model of Toyota Prius without SC

The configuration with one DC/DC converter is the most common configuration as it allows the voltage of the SC model to vary in a wide range while the battery is connected to DC bus and makes the voltage of the battery to stay almost constant. This configuration adds a degree of freedom to the system and makes implementation of many energy management strategies possible without making the configuration too complex.

The complete model which was presented in section 2.2 was chosen as the modelling SC model. Identifying model parameters with a constant current test, being able to represent the behaviour of the SC in both high and low frequencies are the advantages of using this model. As Fig. 2.6 suggests the complete model circuit consists of some elements such as resistant and capacitors. The specifications of these elements need to be identified for the specific SC cell. The SC used for this research is Maxwell BCAP0010. Table 3.1 has the Maxwell BCAP0010 specification which was extracted from manufacturer data sheet.

Table 3.1: Specification of Maxwell BCAP0010 SC Cell

Rated Voltage	Rated Capacity	Series Resistance	Specific Power Density
2.5V	2600F	0.7mΩ	4300 W/kg

Table 3.2: Parameters of Complete Model for Maxwell BCAP0010 SC[1]

R_i	$C(V)$	$T(V)$	R_2	C_2	R_{leak}
0.27 mΩ	$1835 + 613V$ (F)	$1.982 + 0.662V$ (s)	4.5 mΩ	111 F	500 Ω

As the purpose of this research is not sizing the SC model, by assumption we use 100 cells of the Maxwell BCAP010 in the series configuration in our SC model. The complete model parameters for a Maxwell BCAP0010 cell are presented in the Table 3.2. These parameters are validated by different tests in [1]. Also, it should be noted that one the branches of this model is an infinite branch and using the first four elements of that infinite branch gives us enough accuracy we need for this research. The same approach can be found in the literature using the complete model [43].

After modelling the SC model and deciding the configuration for integrating the model with the battery pack of the high-fidelity model, the high-fidelity model of the Toyota Prius vehicle is integrated with SC model. Fig. 3.3 schematically shows this high-fidelity model with SC model, which will be used for all simulations in this study.

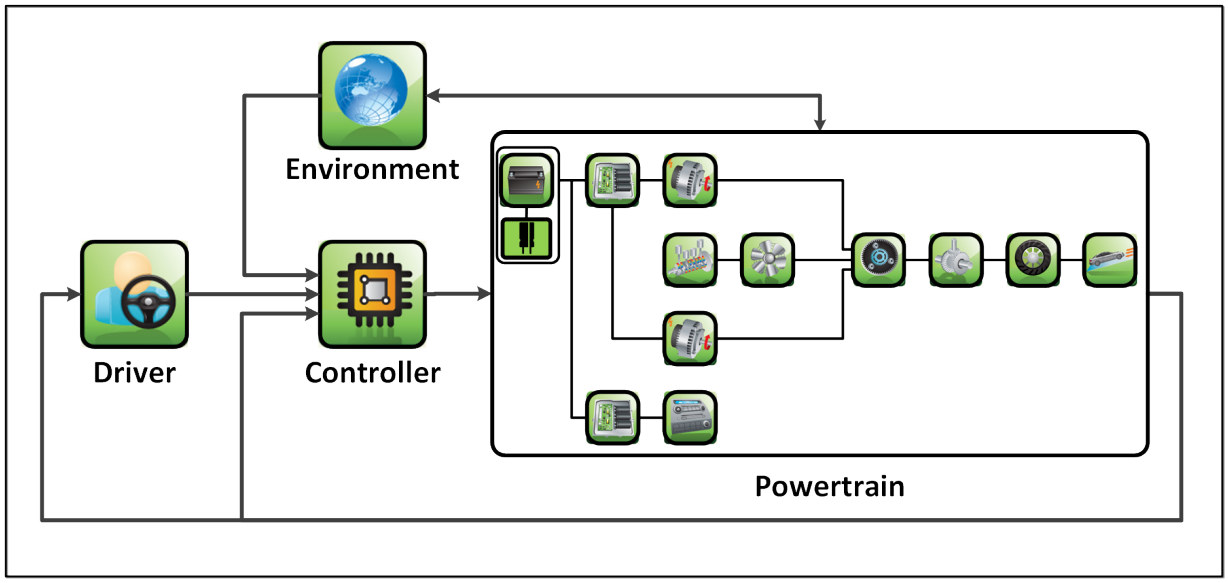

Figure 3.3: Autonomie High-fidelity Model of Toyota Prius with SC

3.3 Control-oriented Model

To design MPC controllers which will be discussed in detail in Chapter 4, a control-oriented model is developed in this section. This control-oriented model is a more computationally efficient model of the main elements.

The main parts of the vehicle that MPC needs to know the behaviour of are Battery, SC, and Engine. Mathematically explaining the behaviour of these parts will be our solution to reduce the complexity of the high-fidelity models of them. Also, it will help us to achieve the real-time implementation of the designed MPCs.

One subject that needs more discussion is the level of accuracy of the control-oriented model. The purpose of developing the control-oriented model is to develop MPC based EMSs. Also, one main goal for these EMSs is to be real-time implementable. Therefore, the level of accuracy of the control-oriented model of the system is constrained by the

rel-time performance of the EMS which is directly related to the computation power of the Electronic Control unit (ECU) of the vehicle. Consequently, the control-oriented model in this study that captures all the dynamics and behaviours of the system and stays within 10% error with the high-fidelity of the system is accurate enough while it is simple enough so the EMS can perform real-time.

As Fig. 3.4 suggests, The battery and SC can be modelled as voltage sources that have internal resistances in series with them. State of the Charge (SOC)), which is a critical factor in decision making in our controllers, is the ratio of the charge in battery or SC to the maximum charge capacity of them. Equation 3.1 explains the dynamic of the battery where SOC_B, V_{OC}, R_B, P_B, and C_B are the battery SOC, open circuit voltage, internal resistance, demanded power, and capacity, respectively. Similarly, equation 3.2 describes the dynamic of the SC, where SOC_{SC}, V_{max}, R_{SC}, P_{SC}, and C_{SC} are the SC SOC, maximum rated voltage, internal resistance, demanded power, and capacity, respectively. Tables 3.3 and 3.1 include the parameters of the control-oriented models for battery and SC extracted from the high-fidelity model.

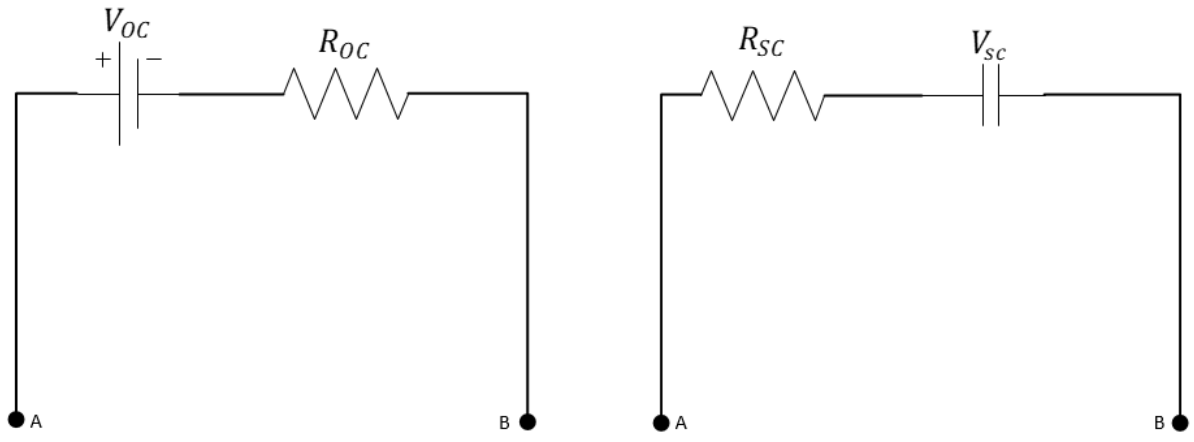

Figure 3.4: Control-oriented Model for Battery (Left) and SC (Right)

$$S\dot{O}C_B = -\frac{V_{OC} - \sqrt{V_{OC}^2 - 4R_B P_B}}{2R_B C_B} \tag{3.1}$$

$$S\dot{O}C_{SC} = -\frac{SOC_{SC} V_{max} - \sqrt{(SOC_{SC} V_{max})^2 - 4R_{SC} P_{SC}}}{2R_{SC} C_{SC} V_{max}} \tag{3.2}$$

Table 3.3: Parameters of Toyota Prius Battery Pack

Voltage (V_{OC})	Resistance	Charge Capacity
207V	0.1Ω	77400 C

The power-split device in the Toyota Prius, which is schematically showed in Fig. 3.1, makes the speed of the engine to be independent of the speed of the vehicle. Hence, power split always makes sure that the engine operates in the optimum (lowest fuel consumption) points among all the possible points with the same power. Fig. 3.5 shows the optimal speeds for different powers.

Fuel consumption of the engine is another critical measurement on which the decisions of the MPC rely. Fig. 3.6 shows the fuel consumption of the engine at different speeds and torques. Knowing the fact that engine always runs at optimum points, a curve can be fitted such that the fuel consumption will be a function of the demanded power of the engine. Equation 3.3 presents this curve and the A, B, and C parameters of this equation are identified in Table 3.4.

$$\dot{m}_f = AP_e + BP_e^{\,2} + CP_e^{\,3} \tag{3.3}$$

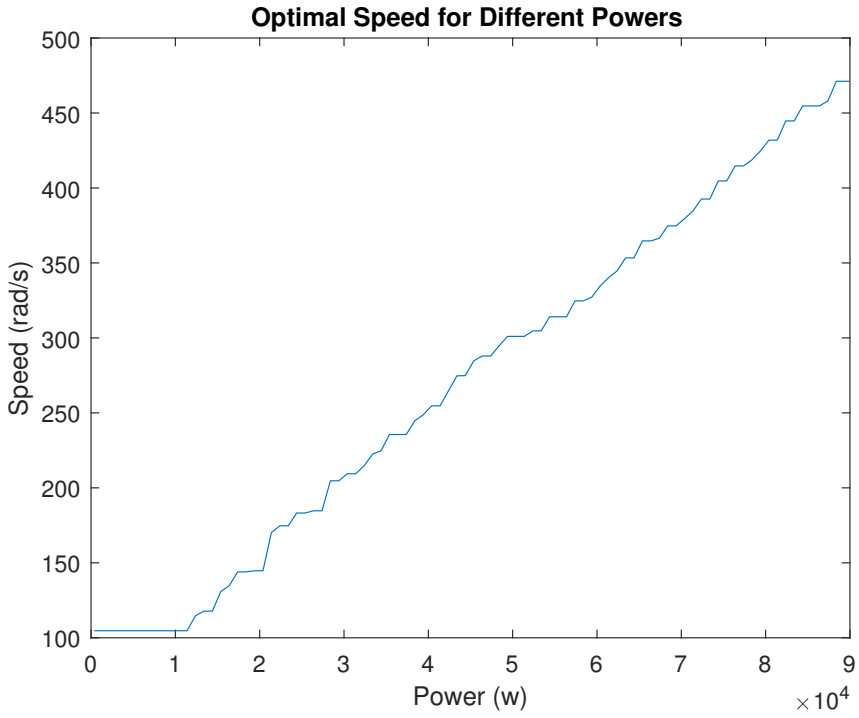

Figure 3.5: Optimal Speed of the Engine for Different Powers

For validating the control-oriented model, a sample experiment was run on both the high-fidelity model and control oriented model to compare the results. Figure 3.7 includes the engine power extracted from an MIL simulation with RBC EMS. The fig. 3.8 shows the battery power for in the MIL simulation. Moreover, Fig. 3.9 is the SC power over time for that simulation. These figures can show the behaviour of the RBC EMS in a sample simulation.

Figures 3.10, 3.11, and 3.13 compare the behavior of high-fidelity and control-oriented model to the same inputs. Fig. 3.10 is the fuel consumption rate for different engine powers and it matches the high fidelity efficiency map of the engine in the high fidelity model. Fig. 3.11 compares the behavior of the high-fidelity and control oriented model in a

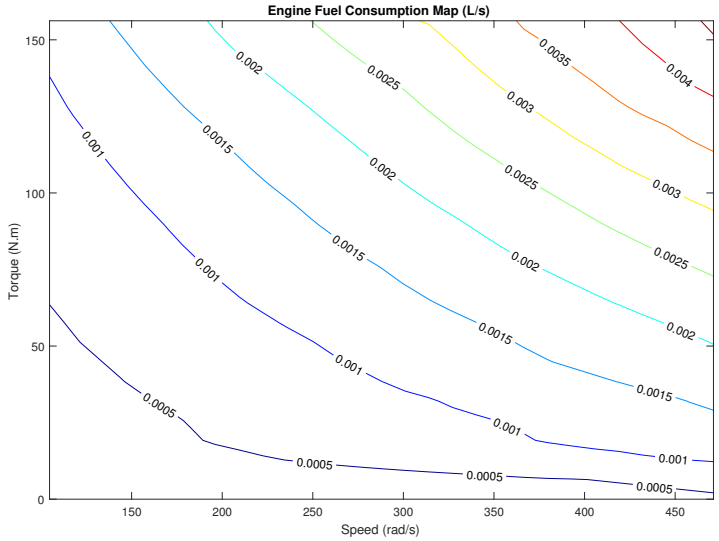

Figure 3.6: Engine Fuel Consumption for Different Torques and Speeds

Table 3.4: Parameters of Fuel Consumption Control-oriented Model in Eq. 3.3

A	B	C
$7.556 \times 10^{-}8$	$-5.971 \times 10^{-}13$	$6.426 \times 10^{-}18$

sample simulation. Fig. 3.13 shows that equation 3.2 successfully captures the behaviour of the high-fidelity of the SC. As these figures show, the control-oriented model can represent the model behaviour with less than 10% error. It should also be mentioned that the error in the SOC of the battery is from the initial states of simulation where the battery is still at ambient temperature. As fig. 3.12 shows, the error in the first 600 seconds of the simulation reaches to 7% and after that, it stays on that level. Therefore, the error in the SOC of the battery is from the transition in temperature of the battery in the high-fidelity and control-oriented model is developed to capture the dominant behaviour of the battery.

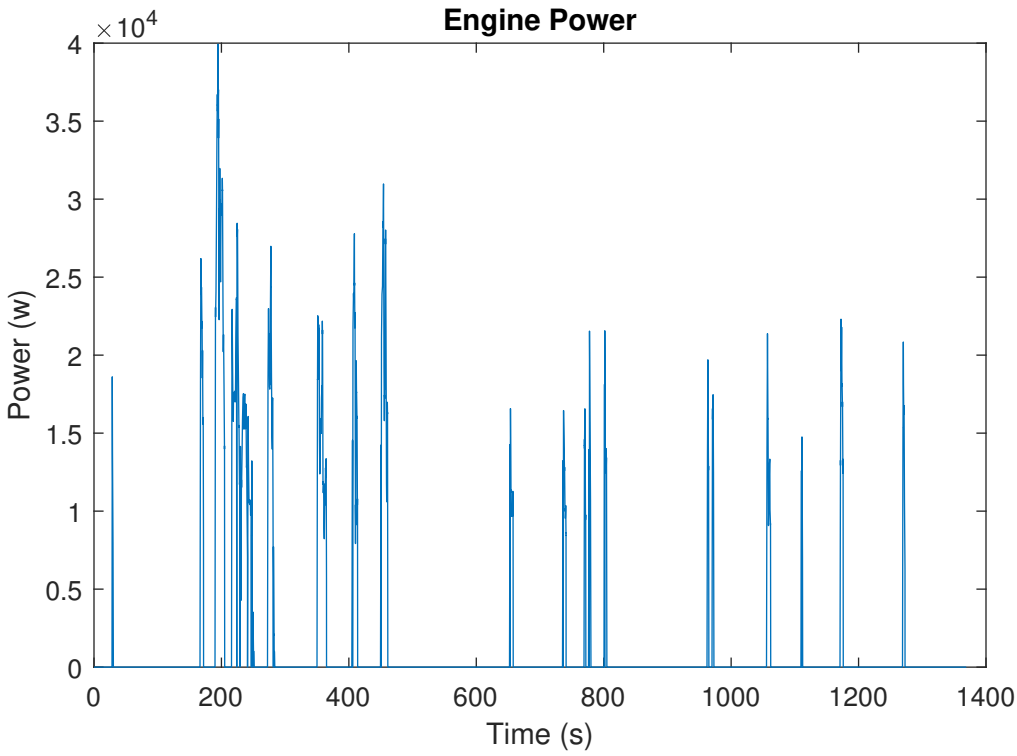

Figure 3.7: Sample Engine Power for Control-oriented Verification

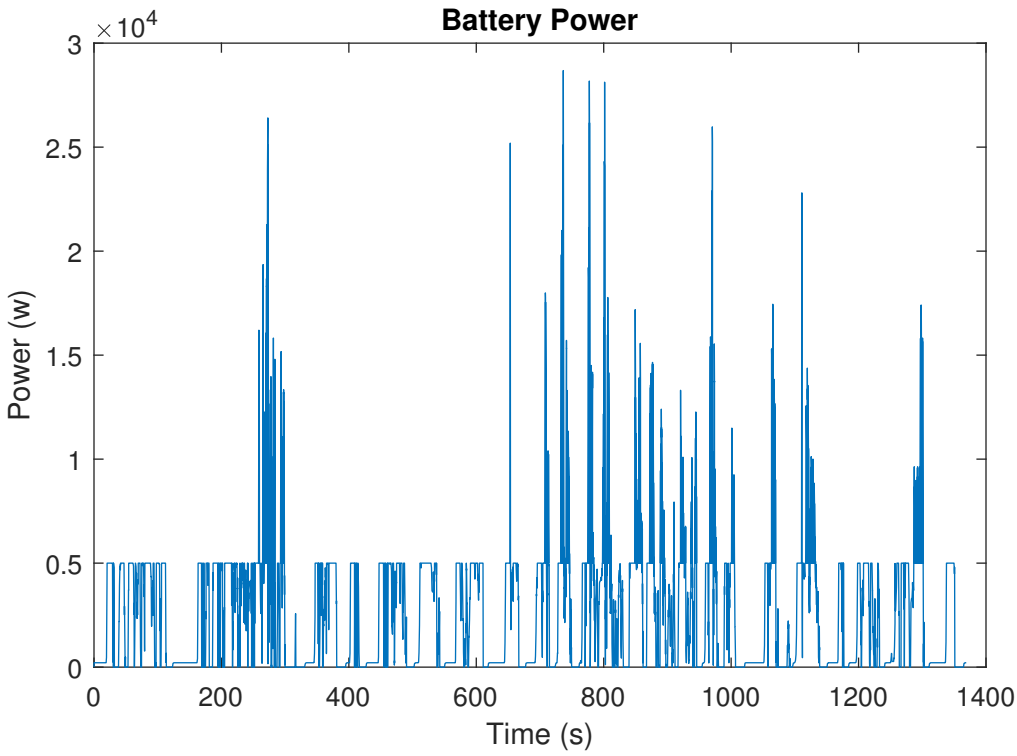

Figure 3.8: Sample Battery Power for Control-oriented Verification

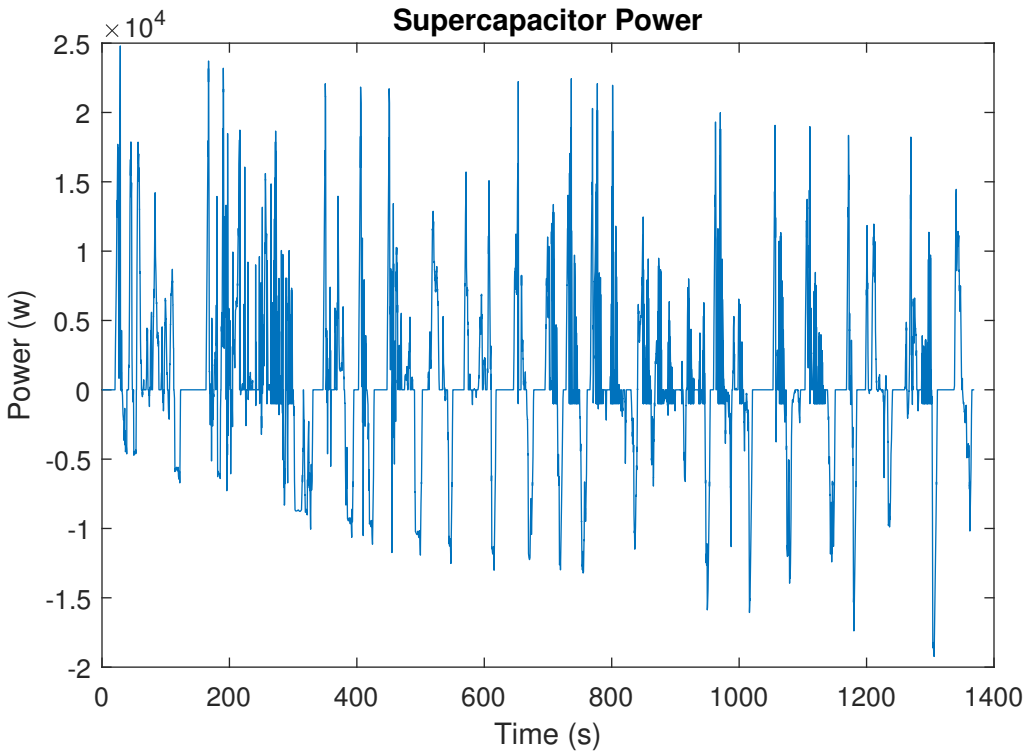

Figure 3.9: Sample SC Power for Control-oriented Verification

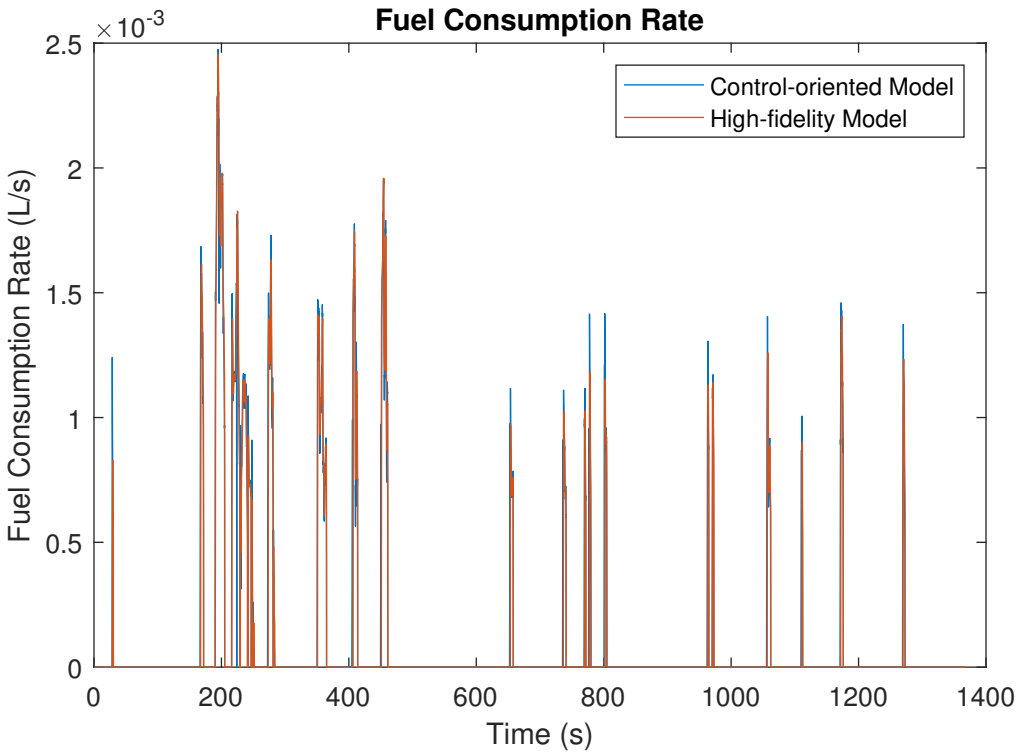

Figure 3.10: Fuel Consumption from High-fidelity and Control-oriented Model Comparison

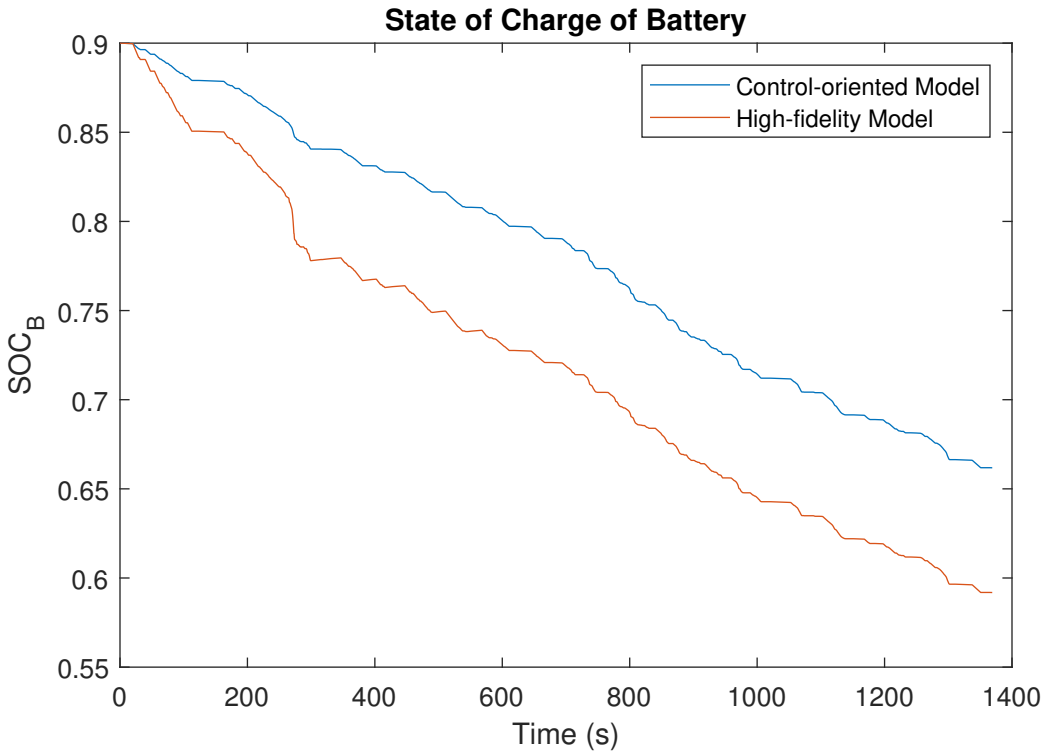

Figure 3.11: Battery High-fidelity and Control-oriented Model Comparison

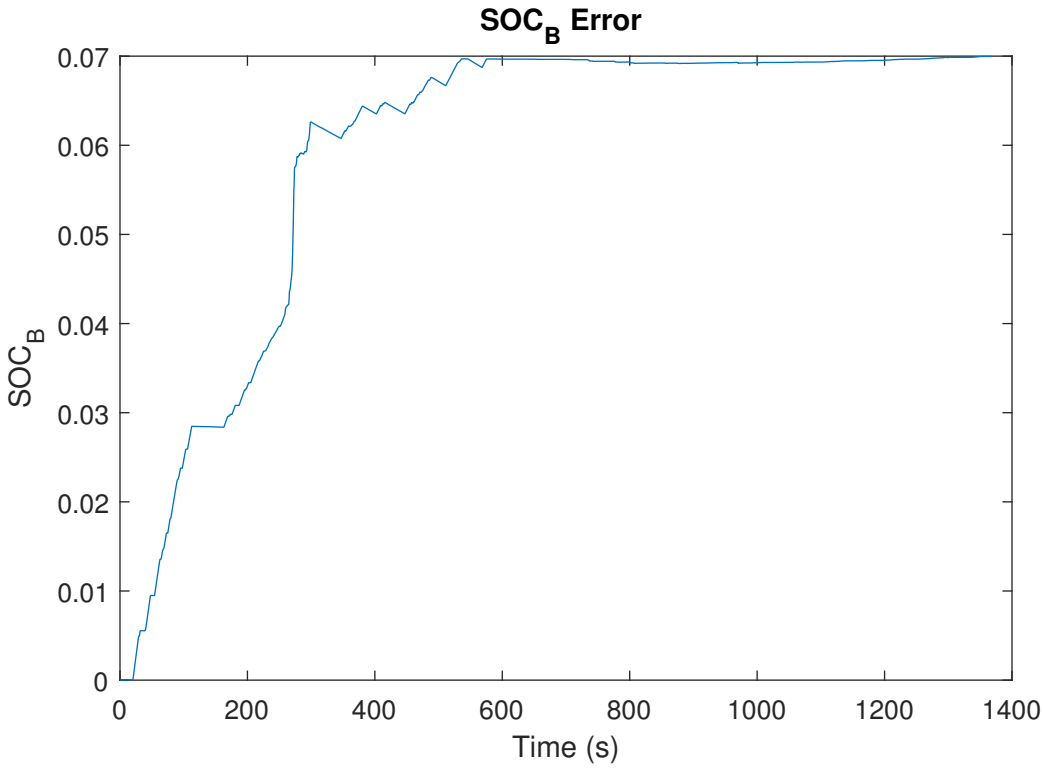

Figure 3.12: Battery High-fidelity and Control-oriented Model Error over Time

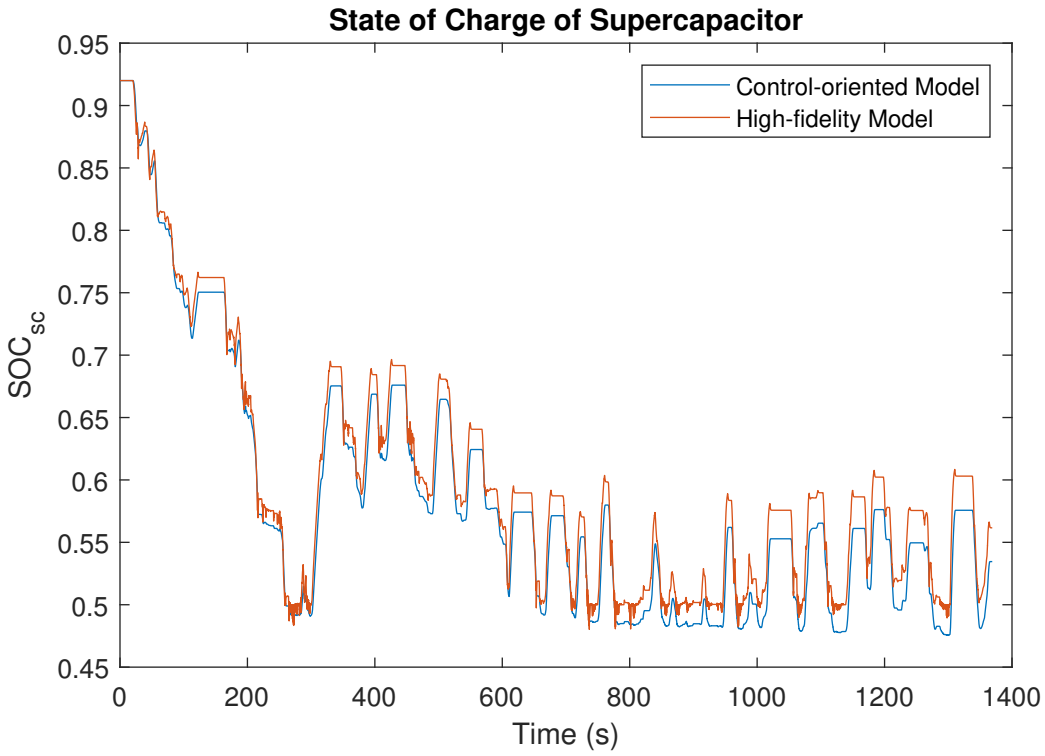

Figure 3.13: SC High-fidelity and Control-oriented Model Comparison

3.4 Summary

This chapter introduces the high-fidelity model of the Toyota Prius. Then, the steps which have been taken to model the SC model are presented. For the purpose of hybridizing the ESS of the vehicle, the most common configuration in the literature was chosen and the elements of that configuration are explained. In the end, the control-oriented model was developed due to the essential parts of the high-fidelity model which will be used in designing different energy management controllers.

Chapter 4

Energy Management Strategy Design

As explained in the previous chapter, EMS of the vehicle is a two-stage controller in which the demanded power from the driver will be divided between the sources of energy in the vehicle: engine, battery, and SC. The higher-level controller in EMS is an RBC from the Autonomie model, and for the lower-level controller, the best RBC introduced in the literature was employed.

In this chapter, MPCs are introduced, and they substitute higher-level and lower-level RBCs. The performance of the designed MPCs in this chapter will be compared with RBCs in the next chapter. Fig. 4.1 schematically shows the relation of the high-level and low-level controllers.

This chapter is organized as follows: in section 4.1, Talks about the high-level and low-level RBCs. Section 4.2 develops the MPC controllers to substitute the RBC. Then, it explains the solver method to solve the optimization problem of NMPC EMS. Finally, Section **??** wraps this chapter with a summary of the architecture of the EMS.

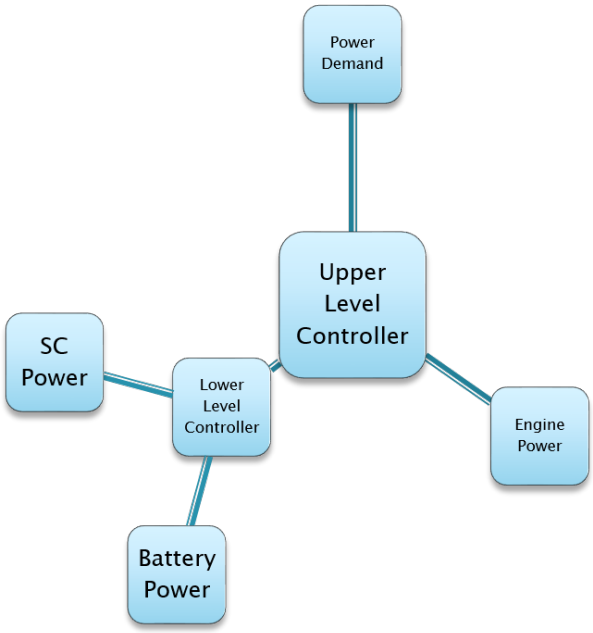

Figure 4.1: Schematic of the High-level and Low-level Controllers Relation

4.1 Rule-based Controllers

RBCs are fast and robust controllers which have commonly been used in different applications due to their simplicity. The RBCs do not provide optimal or sub-optimal solutions to the control problems, but they are computationally efficient and robust to disturbances and uncertainties of the system.

4.1.1 High-level Controller (Engine-HESS)

The role of the high-level controller is to distribute the demanded power between engine and battery. Doing so, this high-level controller exploits the information provided by sensors

and infrastructure as much as possible according to the nature of the controller.

The high-level RBC, which is in the Autonomie model, has the algorithm as Figure 4.2 suggests. High-level RBC is a simple way to distribute the power demand between sources and does not provide the optimal or a sub-optimal answer to the energy management problem.

In this controller, which has a "Charge Depleting Charge Sustaining" strategy, the engine is not turned on unless the SOC is lower than a threshold or engine power demand is higher than the maximum power electric motors can provide. Also, to avoid turning the engine on and off rapidly, the high-level controller makes only turns the engine on when the engine power demand is above zero for a period and turns it off only when the engine power demand is zero for a period.

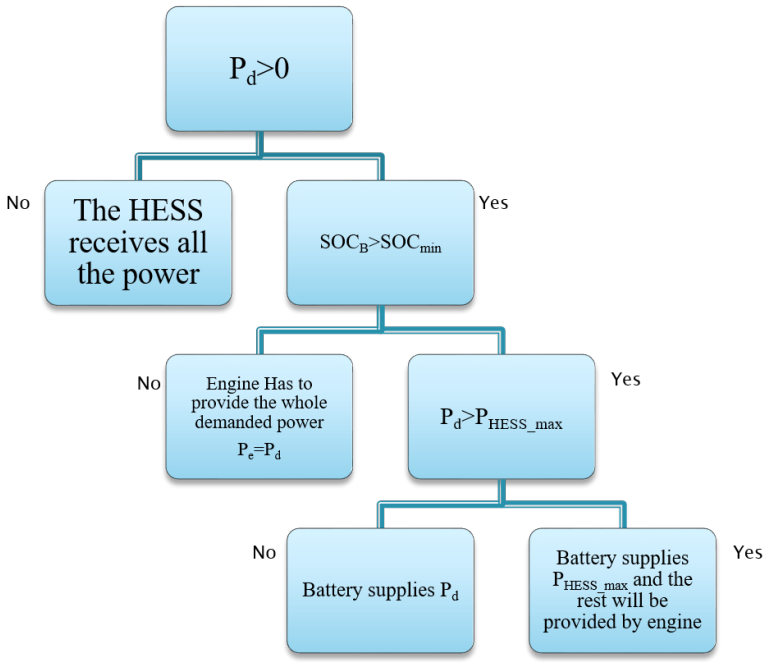

Figure 4.2: Autonomie High-level RBC Algorithm

4.1.2 Low-level Controller (Battery-SC)

The low-level controller is responsible for distributing the HESS power demand between battery and SC. It should be noted that based on the nature of the control strategy, the low-level controller tries to minimize the load on the battery to increase the lifespan of it.

The low-level RBC strategy has an algorithm which is shown in Fig. 4.3. This RBC charges the SC as much as possible in braking situations. While in acceleration, It tries to minimize the load on the battery by assigning the load to the SC as much as possible. As the power density of the SC is dramatically changed when the SOC of it is below 50%, the RBC will not discharge the SC below half. This strategy also has a method to slowly charge the SC from the battery when the SOC of the SC is below 50%. The reason behind this is that the SC should always be possible to take the unpredictable fluctuations in the power demand as it is crucial for the lifespan of the battery.

4.2 Model Predictive Controllers

MPC exploits the future information provided by sensors, infrastructure, or prediction to provide near optimal control input to the system such that the defined cost function for the system is minimized over a prediction horizon.

For this purpose, the controller uses a control-oriented model of the system and the current states from the high-fidelity model to solve the optimization problem. For this study, the author derived a control-oriented model which is introduced and verified in 3.3.

The optimization problem of MPC is usually subject to some constraints too. One of the privileges of using MPC is that this method can solve an optimization problem that is subject to some constraints.

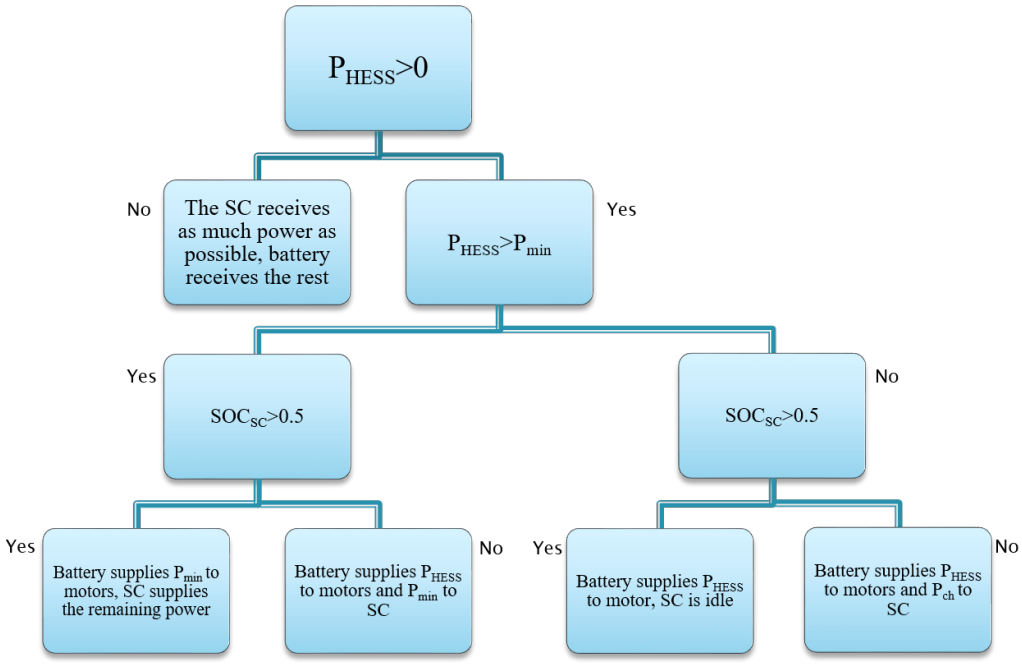

Figure 4.3: Low-level RBC Algorithm [5]

4.2.1 High-level Controller (Engine-HESS)

Equation 4.1 which is a quadratic equation shows the cost function defined for the high-level MPC to substitute the Autonomie RBC controller.

$$\min \int_{t_0}^{t_0+T} L(X,U)dt = \min_{u(t)} \int_{t_0}^{t_0+T} \Big(\omega_1(\dot{m}_f)^2 + \omega_2(SOC_B - SOC_{B,ref})^2\Big)dt \tag{4.1}$$

Which is subject to constraints on input and state as shown in Equations 4.2 and 4.3, respectively.

$$0 \leq P_E \leq P_{E,max} \tag{4.2}$$

$$SOC_{B,min} \leq SOC_B \leq SOC_{B,max} \tag{4.3}$$

Also, the following equation shows the general form of the linearization for the cost function and the constraints to have the LMPC EMS:

$$\dot{X} = AX + BU \tag{4.4}$$

where

$$A = \frac{\partial L(X,U)}{\partial X}, \qquad B = \frac{\partial L(X,U)}{\partial U} \tag{4.5}$$

The cost function defined for the high-level MPC focuses on minimizing the fuel consumption. Also, another objective for this MPC is to make sure that SOC of the battery will follow the reference trajectory. The reference trajectory, $SOC_{B,ref}$, is a linear discharge over the trip length with a constant slope. It should be noted that this trajectory is linear with respect to the length of the trip not the time of the trip. A solver is needed To solve an optimization problem. As the steps of this study need the C-code generation of the solver, solvers implemented in MATLAB such as *fmincon* cannot be used. MPsee NMPC solver developed in [44] was chosen to implement the MPC strategies.

4.2.2 Low-level Controller (Battery-SC)

The cost function for the low-level MPC strategy is presented in Equation 4.6.

$$\min \int_{t_0}^{t_0+T} L(X,U)dt = \min_{u(t)} \int_{t_0}^{t_0+T} \left(\omega_1'(P_B)^2 + \omega_2'(SOC_{SC} - SOC_{SC,ref})^2\right)dt \tag{4.6}$$

This problem is subject to constraints on input and states as shown in Figures 4.7 and 4.8, respectively.

$$P_{SC,min} \leq P_{SC} \leq P_{SC,max} \tag{4.7}$$

$$\begin{aligned} SOC_{B,min} \leq SOC_B \leq SOC_{B,max} \\ SOC_{SC,min} \leq SOC_{SC} \leq SOC_{SC,max} \end{aligned} \tag{4.8}$$

Similarly, the following equation shows the general form of the linearization for the cost function and the constraints to have the LMPC EMS as the low-level controller:

$$\dot{X} = AX + BU \tag{4.9}$$

where

$$A = \frac{\partial L(X,U)}{\partial X}, \qquad B = \frac{\partial L(X,U)}{\partial U} \tag{4.10}$$

The cost function defined for the low-level MPC has mainly one objective and that objective is to minimize Root Mean Square (RMS) of the current of thee battey, I_{RMS}, which is defined in Equation 4.11 [45]. This parameter shows the load on the battery over a cycle. As the current of the battery is only related to the demanded power from the battery, to simplify the cost function, which will reduce the complexity of the problem and increase the computational performance, I_{RMS} is substituted with P_B. The next term in the cost function is to maintain the SOC of the battery at a particular value above the

minimum constraint. The logic behind this term in cost function is to make sure that SC always can participate in providing power. However, it is evident that these two terms are in contradiction. Hence, with tuning the weights if the cost function, a set of weights can be found in a way that can handle the trade-off between these two terms such that the MPC strategy can outperform the benchmark RBCs. Similar to high-level MPC, the MPsee solver is acquired to solve the problem.

$$I_{RMS} = \frac{1}{t_f} \int_0^{t_f} {I_B}^2 dt \tag{4.11}$$

MPsee toolbox is a Newton/GMRES-method-based solver for solving nonlinear optimization problems. In this toolbox the cost function is defined as in equation **??**.

$$J = \Phi(X(t+T) + \int_t^{t+T} L(X(\tau), U(\tau))dt + \sum_{j=1}^{m} \Psi_j(X(t), U(t)) \tag{4.12}$$

where

$$\Psi_j = \begin{cases} 0 & h_j(X,U) \leq 0 \\ r_j h_j(X,U)^2 & h_j(X,U) > 0 \end{cases} \tag{4.13}$$

The $\Psi_j(X(t), U(t))$ matrix defines which constraints are active and which ones are not. MPsee toolbox uses exterior penalty method which means that for each constraint that is active that constraint with a weight, r_j will be added to the cost function.

This toolbox is an iterative method where the optimization problem is solved in each iteration and the constraints will be checked to make sure no constraint is violated. If there is a constraint that is violated the cost function will be updated according to the violated constraints and then the optimization problem will be solved. These iteration steps are

taken to make sure all the constraints are satisfied. Also, there is a maximum number of iteration is defined in the toolbox to make sure that the solver will not be stuck in an infinite loop.

4.3 Summary

First, the high-level RBC which divides demand power between the engine and the ESS was presented. Then the low-level RBC which is responsible for distributing ESS between battery and SC was developed. Finally, these two high-level and low-level RBCs were substituted by NMPCs. Also, by linearization the NMPC equations linear MPCs were developed to compare the performance of the linear MPCs and NMPCs.

Chapter 5

Energy Management Strategy Evaluation

MIL simulation results were exploited to evaluate the designed controllers compared to each other. These results evaluate the performance of the MPCs compared to RBCs. Two objectives that were defined for the MPCs to achieve were reducing fuel consumption and increasing the lifespan of the battery. Results of the simulation for different drive cycles are presented to make sure the performance improvements are not dependant on the driving cycle. Also, to assess the real-time performance of the MPCs HIL tests were implemented. HIL testing measures the time that the controller takes to produce inputs based on the given feedback states.

This chapter is organized as follows: Section 5.1 describes the basics of HIL testing and then presents the HIL tests results. Section 5.2 compares and discusses the results of the MIL simulations over different driving cycles. Finally, Section 5.3 provides a summary of the chapter.

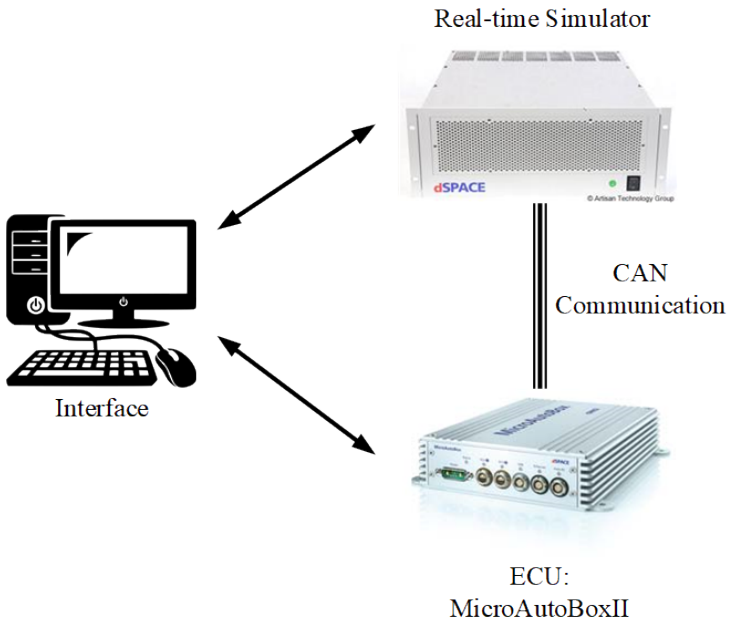

Figure 5.1: Schematic of HIL Setup

5.1 Hardware-in-the-Loop Testing

HIL tests can investigate the real-time performance of the developed controllers. These tests will take the communications of the model and the controller into account. Therefore, the computational costs for the controllers can be measured as a variable that is called turnaround time. Turnaround time is the time that the controllers take to provide the input to the model based on the feedback from the model.

The HIL setup used in this study is schematically shown in Fig. 5.1. This setup consists of: an independent processing unit to store the controller and act as ECU, a real-time simulator to simulate the high-fidelity model, a Controller Area Network (CAN) bus communication for feeding the inputs from the controller to the model and the feedback from the model to the controller, and a Personal Computer (PC) to set up the test and

store the results.

In this study, dSPACE MicroAutoBox II is the controller unit that acts as ECU, dSPACE Real-time Simulator will simulate the model with provided inputs and provides the feedback states, and CAN bus will enable these two components to communicate with each other. More details of the HIL setup components are presented in Table 5.1[46].

Table 5.1: HIL Components Specification

Component	Part	Specification
Real-time Simulator	Hardware	DS-1006 Processor Board
	Processor	DS-1006 Quad-Core AMD, 2.8 GHz
	Memory	1GB local, 4x128 MB global
	I/O	DS-2202
Prototype ECU	Hardware	MicroAutoBox II
	Processor	DS-1401 PowerPC 750GL 900MHz
	Memory	16 MB main, 16 MB nonvolatile
	I/O	DS-1511
Interface	Processor	Core i7, 3.4 GHz
	Memory	16 GB

In order to run the HIL tests, the high-fidelity model and developed controller in Matlab/Simulink are converted into C-codes using dSPACE code generator. These generated codes are uploaded to the dSPACE Real-time Simulator and MicroAutoBox II, respectively. The compiler and code generator of the MicroAutoBox II and Real-time Simulator are rti1401.tlc and rti1006, respectively.

Turnaround time is the time the ECU takes to generate output for a given set of states in each time step. Fig. 5.2 includes a part of the results of the HIL test for a sample drive cycle where the turnaround time for is reported for each time step. The turnaround time results of the HIL tests for different lengths of the prediction horizon for a sample driving cycle are presented in Table 5.2 and Fig. 5.3. Literature suggests that if turnaround time for the ECU of the vehicle is less than $10ms$ the controller can be considered real-time [47]. Therefore, it can be concluded that for the developed MPCs the prediction horizon with the length of $N = 10$ and less are real-time implementable.

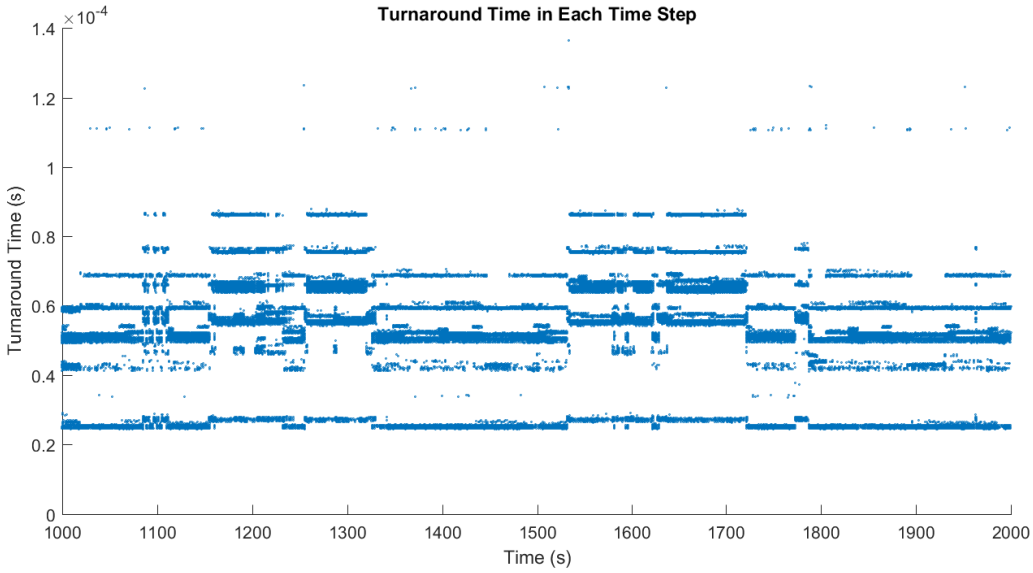

Figure 5.2: Turnaround Times in One HIL Test

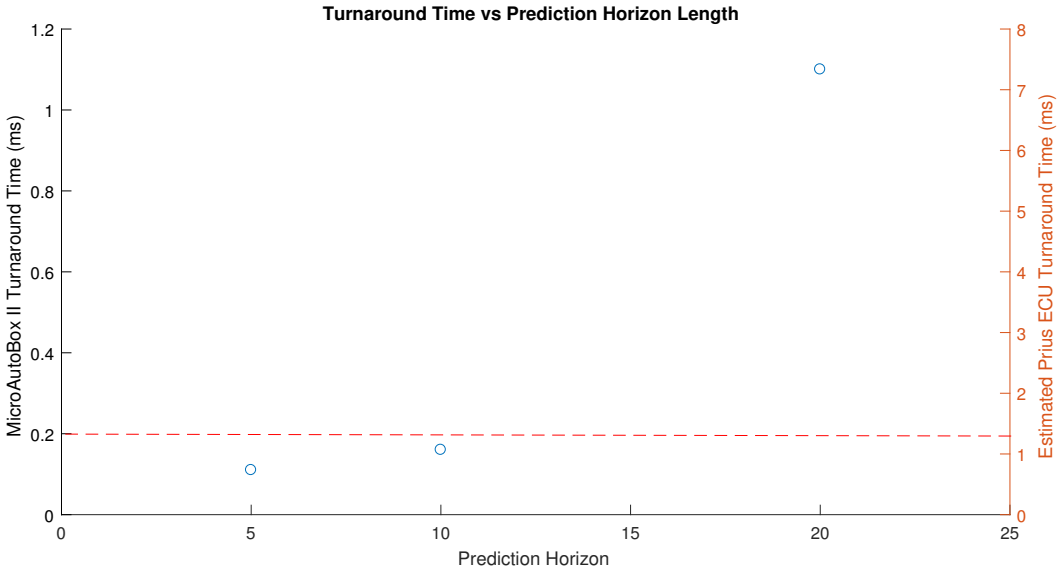

Figure 5.3: Turnaround Time for Different Prediction Horizon Lengths

5.2 Model-in-the-Loop Simulation

MIL simulations are a set of offline experiments which are done mainly to compare the performance of the different energy management strategies to each other. The objectives of these simulations are consist of: (1) comparing the fuel consumption, and (2) comparing the load on the battery which is directly related to the lifespan of the battery [45].

After finding the prediction length ($N = 10$) for the MPCs in order to perform real-time, the set of weights in our MPCs were found to outperform the benchmark RBCs. Again, It should be noted that the MPCs only use the length of the trip in each simulation as the known information. The power demand is assumed to be constant over the prediction horizon in each time-step. So, the MPCs are fallen into the category of frozen-time MPCs.

Three different driving cycles with different were used to make sure the results are not

Table 5.2: Estimated Turnaround Time Based on Measured Turnaround Time

Prediction Horizon Length	MicroAutoBox II Turnaround Time	Estimated Prius ECU Turnaround Time
N=5	0.11ms	0.8ms
N=10	0.16ms	1.1ms
N=20	1.1ms	7.7ms

dependent on the scenario. Also, the driving cycles for the simulations are all long enough, so the SOC of the battery and the end of the simulations is at the minimum level for both RBCs and MPCs.

Tables 5.3 and 5.4 include the performance comparisons of different EMSs regarding the fuel consumption and battery lifespan, respectively. According to these tables, hybridizing ESS of the vehicle with SC model can and implementing MPC strategies can improve the fuel consumption and battery lifespan up to 7.4% and 62%, respectively.

Table 5.3: MIL Simulation Results (Fuel Consumption)

Drive Cycle	Fuel Consumption (L)			Improvement (%)
	RBC	LMPC	NMPC	
2xWLTP	1.28	1.25	1.25	2.3%
3xHWFET	1.24	1.19	1.18	4.8%
3xUDDS	0.81	0.75	0.75	7.4%

Figures 5.4, 5.5, 5.6, 5.9, 5.8, and 5.7 show how the MPC strategies manage to use the

Table 5.4: MIL Simulation Results (Battery Load)

Drive Cycle	Battery Load ($I_{RMS} \times 10^3$)				Improvement (%)
	No SC	RBC	LMPC	NMPC	
2xWLTP	2.33	1.39	1.28	1.27	46%
3xHWFET	1.73	1.38	1.20	1.19	31%
3xUDDS	2.61	1.37	1.00	1.00	62%

engine more wisely over the driving cycle, exploiting only the length of the trip as known future information, to achieve: (1) less fuel consumption (2) less load on the battery. Following paragraphs discuss fuel consumption and battery load in each driving cycle.

First drive cycle is 2xWLTP which has both high speed and low speed sections. This cycle has repetitive acceleration and braking. Figure 5.4 shows the fuel consumption in 2xWLTP cycle. MPC EMS exploits the future information to reduce fuel consumption. The key factor in improving the fuel consumption by NMPC is trip length information that motivates the EMS to save electrical energy for later in the trip. Moreover, as shown in Fig. 5.7, in this driving cycle, NMPC takes advantage of the SC to absorb all the energy in barking and accelerating the vehicle in acceleration. The NMPC makes this decision based on fact that internal resistance of the SC is lower and this can waste less energy as heat.

Second drive cycle is 3xHWFET which is a highway cycle that has less intense braking and acceleration compared to other drive cycles used in this study. In this drive cycle, the fuel consumption improvement is more compared to the first drive cycle due to the fact that this is a highway cycle and the EMS is more likely to use engine more often.

Therefore, the NMPC EMS outperforms the RBC EMS by preventing the SOC of the battery to reach the minimum limit so engine can always be in a region that uses less fuel. Fig. 5.5 includes more detail on the decisions of the different EMSs. Simultaneously, as shown in Fig. 5.8, the NMPC EMS utilizes the SC in the speed fluctuations to help the battery to have less load. This improves the lifespan of the battery by **31%** compared to the RBC EMS for PHEV without SC. The improvement in the battery load is less in this driving cycle compared to other drive cycles used in this study as this cycle has less fluctuations.

Last drive cycle is 3xUDDS which has the most intensive braking and acceleration among the three cycles. Fig. 5.6 shows the fuel consumption in this drive cycle. This is the longest drive cycle and this leads to more fuel consumption as RBC EMS uses all the electric energy as soon as possible and employs a charge sustaining policy after that. On the other hand, NMPC takes advantage of the trip length information to keep the engine operating under low loads over the whole trip and this improves the fuel consumption. At the same time, the NMPC uses the SC to prevent loading the battery and improves the lifespan of the battery by reducing the load of the battery. As Fig. 5.9 shows, RBC outperforms the NMPC in the first 1000 seconds, but the NMPC optimmizes the behaviour of the system over the whole trip exploiting the trip length information.

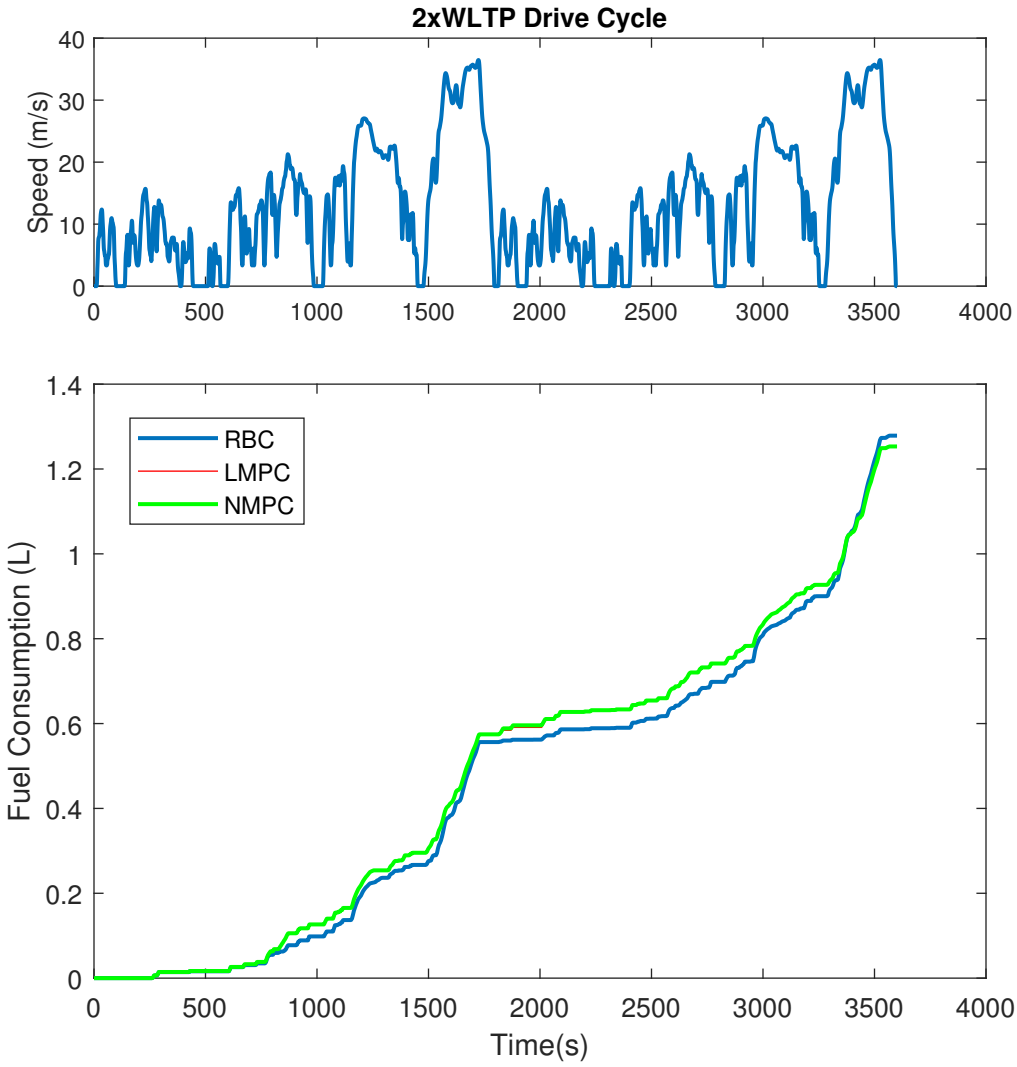

Figure 5.4: Fuel Consumption Comparison for 2xWLTP Drive Cycle

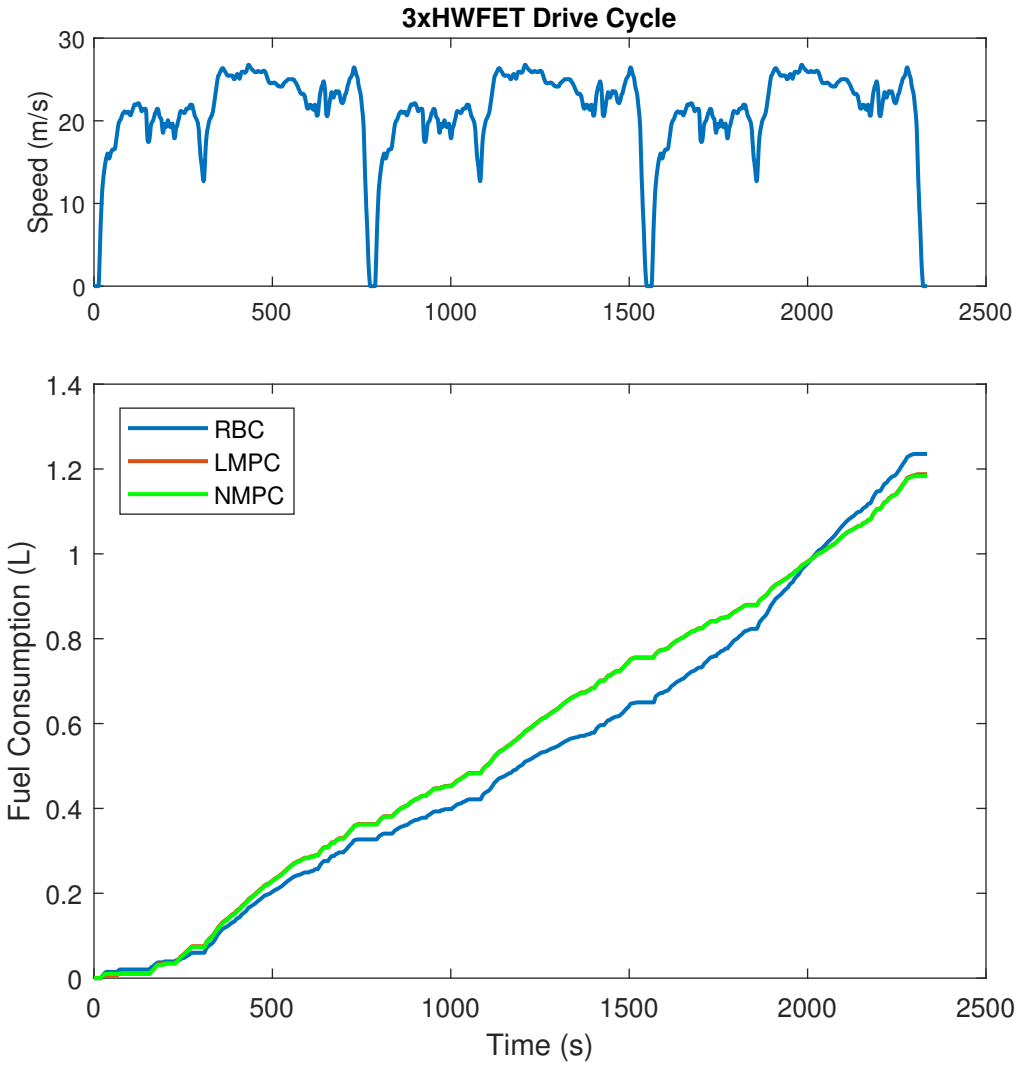

Figure 5.5: Fuel Consumption Comparison for 3xHWFET Drive Cycle

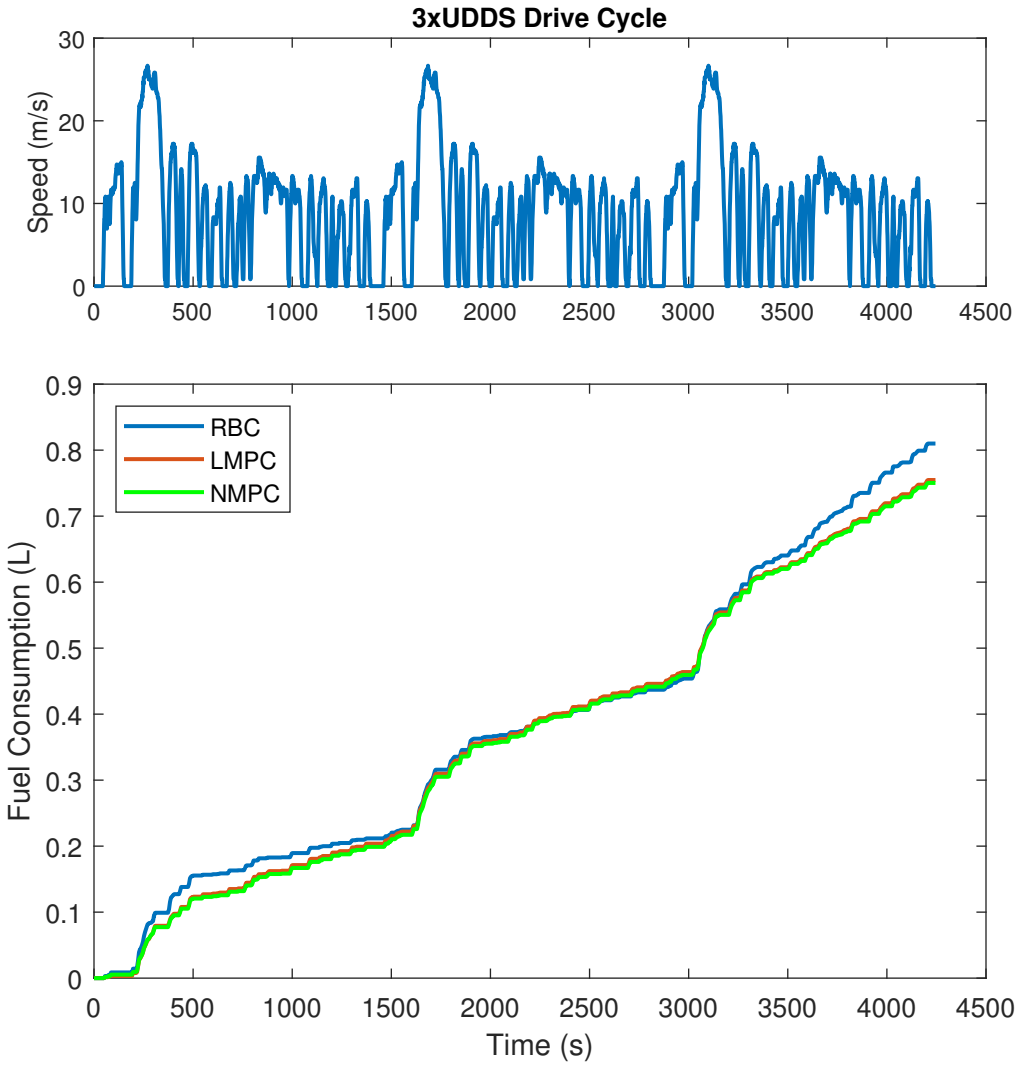

Figure 5.6: Fuel Consumption Comparison for 3xUDDS Drive Cycle

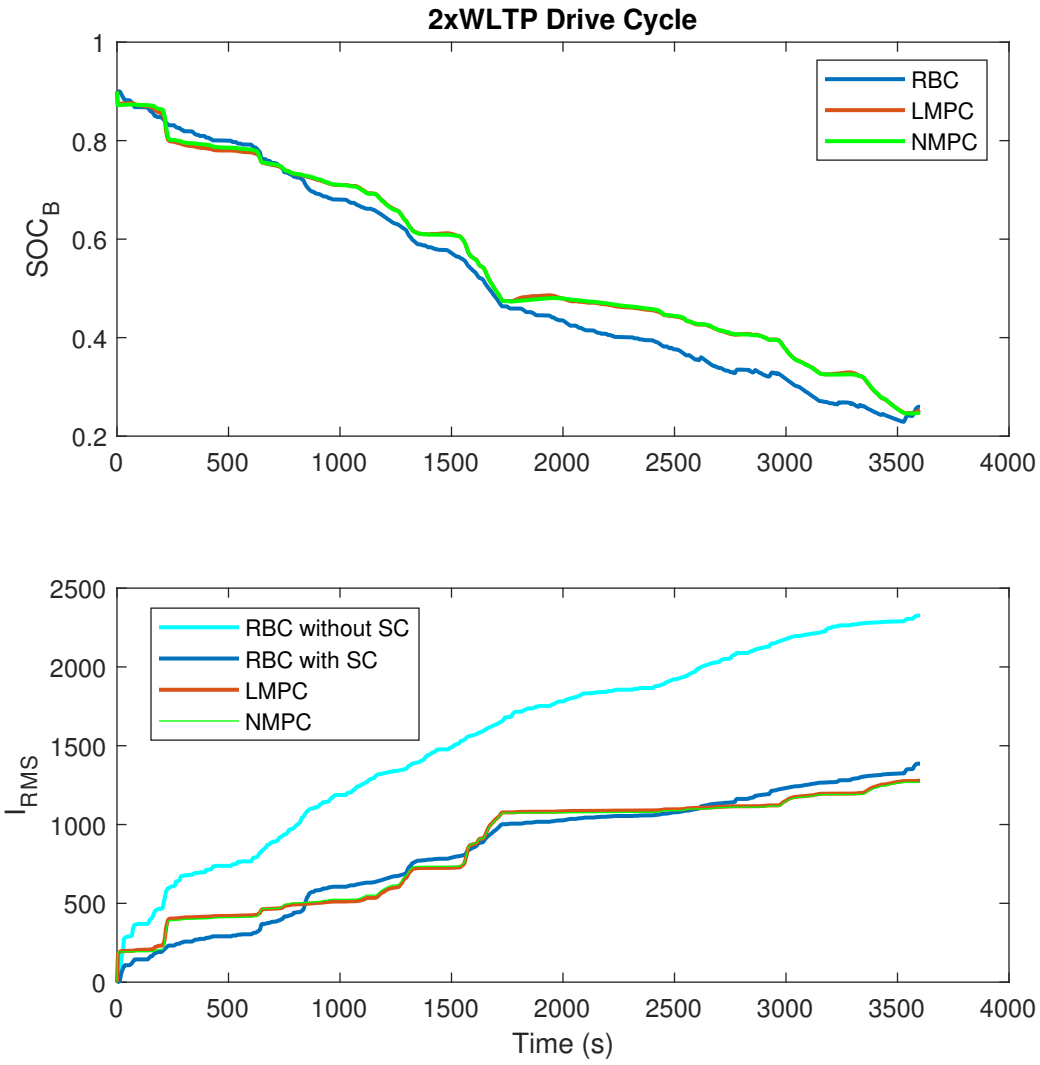

Figure 5.7: Battery Load Comparison for 2xWLTP Drive Cycle

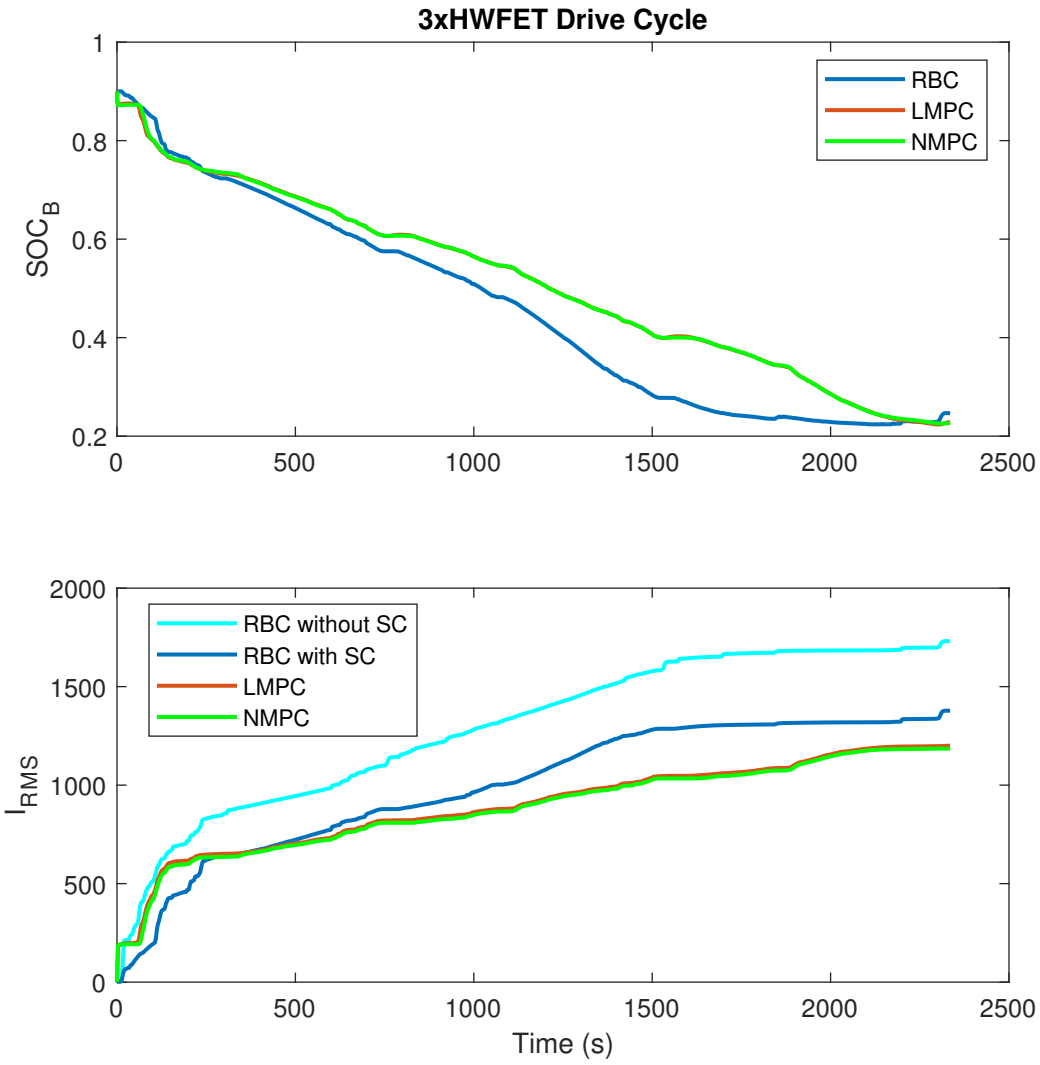

Figure 5.8: Battery Load Comparison for 3xHWFET Drive Cycle

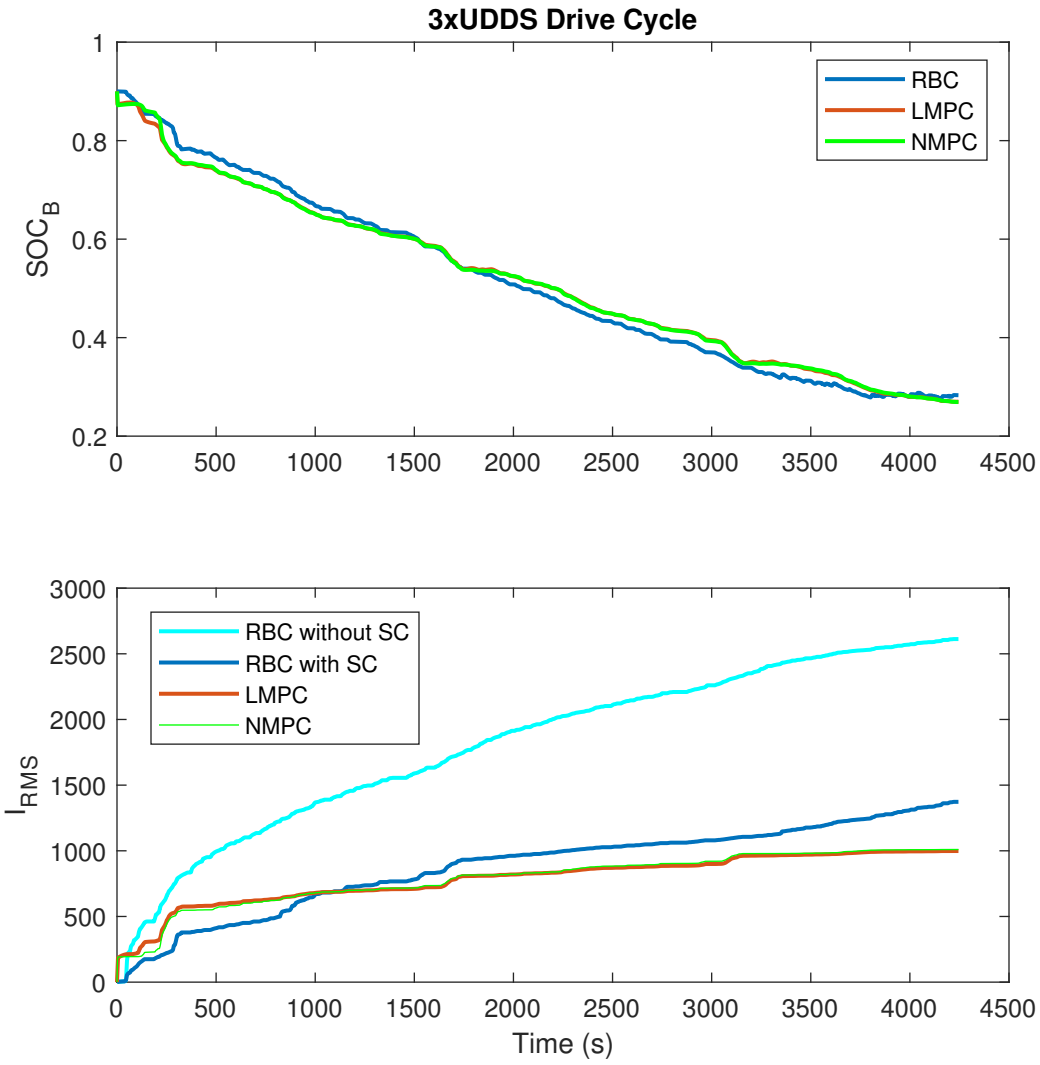

Figure 5.9: Battery Load Comparison for 3xUUDS Drive Cycle

5.3 Summary

Results of both HIL and MIL tests were presented in this chapter. HIL tests' goal was to find out the prediction horizon length so the controllers can produce closer solutions to the optimal global solution for the problem while they meet the criteria to be real-time implementable. The MIL simulations highlighted the performance improvements that can be achieved using the MPC strategies compared to benchmark RBC strategies. The MIL simulations over different driving cycles reassured us that the MPC performance is robust to the unpredictable nature of the driver behaviour.

Chapter 6

Conclusion and Future Work

Real-time model predictive control of Toyota Prius PHEV with SC was presented. SC model with compatibility with automotive applications was modelled and parameters of the model were identified. The integration of the PHEV high-fidelity model and SC model was used as baseline for all the experiments.

HIL setup was used to check the real-time performance of the proposed control strategies and to find the region inside which the MPC strategies will be considered real-time. dSPACE hardware and software were used to achieve these tests.

MIL simulations for different scenarios showed that the MPC strategies with exploiting the length of the trip as the only known future information can outperform the benchmark RBC strategies dramatically. Also, the results show that the improvements are robust to the unpredictable nature of the driver behavior.

This study concludes adding SC to the Toyota Prius PHEV can reduce the load of the battery up to **47%**. Moreover, utilizing MPC strategy for EMS of the system can improve the fuel consumption up to **7.4%** and the battery lifespan up to **62%** compared to PHEV

without SC.

The potentials of improvement based on exploiting more future driving information into the MPCs and combining the high-level and low-level controllers is still under investigation and are left out to the next steps of this study.

6.1 Contributions

The major contributions of this research are as follows:

- This thesis developed real-time NMPC for PHEVs with SC for the first time. The real-time performance of the proposed controllers has been guaranteed through HIL tests.
- A novel state of the art two-stage controller approach MPC strategies was established for the first time
- Both fuel consumption and battery lifespan improvements were achieved with MPC strategies for the first time

6.2 Future Steps

The next steps of this study for further improvements are as follows:

- Combining the high-level and low-level controller to a MIMO controller
- Studying the potential improvements with using full knowledge of the future

- Developing a neural network future velocity predictor model to predict the behavior of the driver
- taking more steps in robustness and stability analysis
- Investigating the performance of the MPC strategies with different optimization solvers
- Performing component-in-the-loop tests with real engine, battery, and SC model

References

[1] E. Tironi and V. Musolino, "Supercapacitor characterization in power electronic applications: Proposal of a new model," in *Clean Electrical Power, 2009 International Conference on*, pp. 376–382, IEEE, 2009.

[2] S. Buller, E. Karden, D. Kok, and R. De Doncker, "Modeling the dynamic behavior of supercapacitors using impedance spectroscopy," in *Industry Applications Conference, 2001. Thirty-Sixth IAS Annual Meeting. Conference Record of the 2001 IEEE*, vol. 4, pp. 2500–2504, IEEE, 2001.

[3] R. Faranda, M. Gallina, and D. Son, "A new simplified model of double-layer capacitors," in *Clean Electrical Power, 2007. ICCEP'07. International Conference on*, pp. 706–710, IEEE, 2007.

[4] Y. Huang, H. Wang, A. Khajepour, H. He, and J. Ji, "Model predictive control power management strategies for hevs: A review," *Journal of Power Sources*, vol. 341, pp. 91–106, 2017.

[5] J. P. Trovão, P. G. Pereirinha, H. M. Jorge, and C. H. Antunes, "A multi-level energy management system for multi-source electric vehicles–an integrated rule-based meta-heuristic approach," *Applied Energy*, vol. 105, pp. 304–318, 2013.

[6] J. Woodcock, P. Edwards, C. Tonne, B. G. Armstrong, O. Ashiru, D. Banister, S. Beevers, Z. Chalabi, Z. Chowdhury, A. Cohen, *et al.*, "Public health benefits of strategies to reduce greenhouse-gas emissions: urban land transport," *The Lancet*, vol. 374, no. 9705, pp. 1930–1943, 2009.

[7] C. Kennedy, J. Steinberger, B. Gasson, Y. Hansen, T. Hillman, M. Havranek, D. Pataki, A. Phdungsilp, A. Ramaswami, and G. V. Mendez, "Greenhouse gas emissions from global cities," 2009.

[8] B. Metz, O. R. Davidson, P. R. Bosch, R. Dave, and L. A. Meyer, "Contribution of working group iii to the fourth assessment report of the intergovernmental panel on climate change, 2007," 2007.

[9] A. Elgowainy, A. Burnham, M. Wang, J. Molburg, and A. Rousseau, "Well-to-wheels energy use and greenhouse gas emissions of plug-in hybrid electric vehicles," *SAE International Journal of Fuels and Lubricants*, vol. 2, no. 1, pp. 627–644, 2009.

[10] A. Elgowainy, J. Han, L. Poch, M. Wang, A. Vyas, M. Mahalik, and A. Rousseau, "Well-to-wheels analysis of energy use and greenhouse gas emissions of plug-in hybrid electric vehicles.," tech. rep., Argonne National Lab.(ANL), Argonne, IL (United States), 2010.

[11] H. Ma, F. Balthasar, N. Tait, X. Riera-Palou, and A. Harrison, "A new comparison between the life cycle greenhouse gas emissions of battery electric vehicles and internal combustion vehicles," *Energy policy*, vol. 44, pp. 160–173, 2012.

[12] A. J. Markel and A. Simpson, *Plug-in hybrid electric vehicle energy storage system design*. National Renewable Energy Laboratory, 2006.

[13] J. M. Miller, "Energy storage technology markets and applications: ultracapacitors in combination with lithium-ion," in *Power Electronics, 2007. ICPE'07. 7th Internatonal Conference on*, pp. 16–22, IEEE, 2007.

[14] M. Winter and R. J. Brodd, "What are batteries, fuel cells, and supercapacitors?," 2004.

[15] M. Vajedi and N. L. Azad, "Ecological adaptive cruise controller for plug-in hybrid electric vehicles using nonlinear model predictive control," *IEEE Transactions on Intelligent Transportation Systems*, vol. 17, no. 1, pp. 113–122, 2016.

[16] A. Mozaffari, N. L. Azad, and J. K. Hedrick, "A nonlinear model predictive controller with multiagent online optimizer for automotive cold-start hydrocarbon emission reduction," *IEEE Transactions on Vehicular Technology*, vol. 65, no. 6, pp. 4548–4563, 2016.

[17] J. Cao and A. Emadi, "A new battery/ultracapacitor hybrid energy storage system for electric, hybrid, and plug-in hybrid electric vehicles," *IEEE Transactions on power electronics*, vol. 27, no. 1, pp. 122–132, 2012.

[18] S. M. Lukic, S. G. Wirasingha, F. Rodriguez, J. Cao, and A. Emadi, "Power management of an ultracapacitor/battery hybrid energy storage system in an hev," in *Vehicle Power and Propulsion Conference, 2006. VPPC'06. IEEE*, pp. 1–6, IEEE, 2006.

[19] M. Ortúzar, J. Moreno, and J. Dixon, "Ultracapacitor-based auxiliary energy system for an electric vehicle: Implementation and evaluation," *IEEE Transactions on industrial electronics*, vol. 54, no. 4, pp. 2147–2156, 2007.

[20] A. Di Napoli, F. Crescimbini, F. G. Capponi, and L. Solero, "Control strategy for multiple input dc-dc power converters devoted to hybrid vehicle propulsion systems," in *Proc. IEEE ISIE*, vol. 3, pp. 1036–1041, 2002.

[21] A. Di Napoli, F. Crescimbini, L. Solero, F. Caricchi, and F. G. Capponi, "Multiple-input dc-dc power converter for power-flow management in hybrid vehicles," in *Industry Applications Conference, 2002. 37th IAS Annual Meeting. Conference Record of the*, vol. 3, pp. 1578–1585, IEEE, 2002.

[22] R. Kötz and M. Carlen, "Principles and applications of electrochemical capacitors," *Electrochimica acta*, vol. 45, no. 15-16, pp. 2483–2498, 2000.

[23] P. Kurzweil, B. Frenzel, and R. Gallay, "Capacitance characterization methods and ageing behaviour of supercapacitors," in *Proc. 15th International Seminar On Double Layer Capacitors, Deerfield Beach, FL., USA*, pp. 14–25, 2005.

[24] M. Jamshidi and A. Zilouchian, *Intelligent control systems using soft computing methodologies*. CRC press, 2001.

[25] J. S. Albus, "Outline for a theory of intelligence," *IEEE Transactions on Systems, Man, and Cybernetics*, vol. 21, no. 3, pp. 473–509, 1991.

[26] Y. Wang and S. Boyd, "Fast model predictive control using online optimization," in *Proceedings IFAC world congress*, pp. 6974–6997, Citeseer, 2008.

[27] H. Seguchi and T. Ohtsuka, "Nonlinear receding horizon control of an underactuated hovercraft," *International Journal of Robust and Nonlinear Control: IFAC-Affiliated Journal*, vol. 13, no. 3-4, pp. 381–398, 2003.

[28] K. I. Kouramas, C. Panos, N. P. Faísca, and E. N. Pistikopoulos, "An algorithm for robust explicit/multi-parametric model predictive control," *Automatica*, vol. 49, no. 2, pp. 381–389, 2013.

[29] F. Allgöwer and A. Zheng, *Nonlinear model predictive control*, vol. 26. Birkhäuser, 2012.

[30] H. Banvait, J. Hu, and Y. Chen, "Energy management control of plug-in hybrid electric vehicle using hybrid dynamical systems," *IEEE Transactions on Intelligent Transportation Systems*, 2013.

[31] S. Zhang, R. Xiong, and F. Sun, "Model predictive control for power management in a plug-in hybrid electric vehicle with a hybrid energy storage system," *Applied Energy*, vol. 185, pp. 1654–1662, 2017.

[32] S. Di Cairano, D. Bernardini, A. Bemporad, and I. V. Kolmanovsky, "Stochastic mpc with learning for driver-predictive vehicle control and its application to hev energy management.," *IEEE Trans. Contr. Sys. Techn.*, vol. 22, no. 3, pp. 1018–1031, 2014.

[33] D. Rotenberg, A. Vahidi, and I. Kolmanovsky, "Ultracapacitor assisted powertrains: Modeling, control, sizing, and the impact on fuel economy," *IEEE Transactions on Control Systems Technology*, vol. 19, no. 3, pp. 576–589, 2011.

[34] C. Sun, X. Hu, S. J. Moura, and F. Sun, "Velocity predictors for predictive energy management in hybrid electric vehicles.," *IEEE Trans. Contr. Sys. Techn.*, vol. 23, no. 3, pp. 1197–1204, 2015.

[35] P. Zhang, F. Yan, and C. Du, "A comprehensive analysis of energy management strategies for hybrid electric vehicles based on bibliometrics," *Renewable and Sustainable Energy Reviews*, vol. 48, pp. 88–104, 2015.

[36] D. F. Opila, X. Wang, R. McGee, and J. Grizzle, "Real-time implementation and hardware testing of a hybrid vehicle energy management controller based on stochastic dynamic programming," *Journal of dynamic systems, measurement, and control*, vol. 135, no. 2, p. 021002, 2013.

[37] J. Tang, L. Guo, B. Gao, Q. Liu, S. Yu, and H. Chen, "Energy management of a parallel hybrid electric vehicle with cvt using model predictive control," in *Control Conference (CCC), 2016 35th Chinese*, pp. 4396–4401, IEEE, 2016.

[38] H. Borhan, A. Vahidi, A. M. Phillips, M. L. Kuang, I. V. Kolmanovsky, and S. Di Cairano, "Mpc-based energy management of a power-split hybrid electric vehicle," *IEEE Transactions on Control Systems Technology*, vol. 20, no. 3, pp. 593–603, 2012.

[39] Y. L. Murphey, J. Park, Z. Chen, M. L. Kuang, M. A. Masrur, and A. M. Phillips, "Intelligent hybrid vehicle power controlpart i: Machine learning of optimal vehicle power," *IEEE Transactions on Vehicular Technology*, vol. 61, no. 8, pp. 3519–3530, 2012.

[40] X. Zeng and J. Wang, "A two-level stochastic approach to optimize the energy management strategy for fixed-route hybrid electric vehicles," *Mechatronics*, vol. 38, pp. 93–102, 2016.

[41] M. T. Hagan, H. B. Demuth, M. H. Beale, and O. De Jesús, *Neural network design*, vol. 20. Pws Pub. Boston, 1996.

[42] A. Taghavipour, R. Masoudi, N. L. Azad, and J. McPhee, "High-fidelity modeling of a power-split plug-in hybrid electric powertrain for control performance evaluation,"

in *ASME 2013 International Design Engineering Technical Conferences and Computers and Information in Engineering Conference*, pp. V001T01A008–V001T01A008, American Society of Mechanical Engineers, 2013.

[43] A. Abuaish and M. Kazerani, "Comparative evaluation of partially-decoupled battery-supercapacitor hess topologies for evs from battery pack capacity fading viewpoint," in *Transportation Electrification Conference and Expo (ITEC), 2016 IEEE*, pp. 1–8, IEEE, 2016.

[44] S. Tajeddin, "Automatic code generation of real-time nonlinear model predictive control for plug-in hybrid electric vehicle intelligent cruise controllers," Master's thesis, University of Waterloo, 2016.

[45] S. Ermon, Y. Xue, C. Gomes, and B. Selman, "Learning policies for battery usage optimization in electric vehicles," *Machine Learning*, vol. 92, no. 1, pp. 177–194, 2013.

[46] M. Vajedi, "Real-time optimal control of a plug-in hybrid electric vehicle using trip information," 2016.

[47] M. Vukov, W. Van Loock, B. Houska, H. J. Ferreau, J. Swevers, and M. Diehl, "Experimental validation of nonlinear mpc on an overhead crane using automatic code generation," in *American Control Conference (ACC), 2012*, pp. 6264–6269, IEEE, 2012.

[48] P. Golchoubian and N. L. Azad, "Real-time nonlinear model predictive control of a battery–supercapacitor hybrid energy storage system in electric vehicles," *IEEE Transactions on Vehicular Technology*, vol. 66, no. 11, pp. 9678–9688, 2017.

[49] P. Golchoubian, "Real-time energy management of a battery electric vehicle hybridized with supercapacitor," Master's thesis, University of Waterloo, 2017.